MVJ College of Engineering, Bengaluru
(An Autonomous Institute)
Affiliated to VTU, Belagavi, Approved by AICTE, New Delhi,
Recognized by UGC with 12(f) & 12 (B), Accredited by NBA & NAAC

DEPARTMENT OF AEROSPACE ENGINEERING

CERTIFICATE

Certified that the mini project work titled 'Heat shield deployment system' is carried out by **ADITYA S (1MJ19AS003), KIRAN KB (1MJ19AS020), PAWAR VAIBHAV BHUPENDRA (1MJ19AS029)** and **SATHVIK SWAMY (1MJ19AS039)** who are confide students of MVJ College of Engineering, Bengaluru, in partial fulfilment for the award of Degree of Bachelor of Engineering in Aerospace Engineering of the Visvesvaraya Technological University, Belagavi during the year 2021-2022. It is certified that all corrections/suggestions indicated for the Internal Assessment have been incorporated in the mini project report deposited in the departmental library. The mini project report has been approved as it satisfies the academic requirements in respect of mini project work prescribed by the institution for the said Degree.

Signature of Guide	**Signature of Head of the Department**	**Signature of Principal**
Mr. Narendra Singh Maurya	**Prof. S C Gupta**	**Dr. P Mahabaleswarappa**

External Viva

Name of Examiners	**Signature with Date**
1	
2	

MVJ College of Engineering, Bengaluru
(An Autonomous Institute)
Affiliated to VTU, Belagavi, Approved by AICTE, New Delhi,
Recognized by UGC with 12(f) & 12 (B), Accredited by NBA & NAAC

DEPARTMENT OF AEROSPACE ENGINEERING

DECLARATION

We, **ADITYA S (1MJ19AS003), KIRAN KB (1MJ19AS020), PAWAR VAIBHAV BHUPENDRA (1MJ19AS029)** and **SATHVIK SWAMY (1MJ19AS039)** students of sixth semester B.E., Department of Aerospace Engineering, MVJ College of Engineering, Bengaluru, hereby declare that the mini project titled 'Heat shield deployment system' has been carried out by us and submitted in partial fulfilment for the award of Degree of Bachelor of Engineering in Aerospace Engineering during the year 2021-2022. Further we declare that the content of the dissertation has not been submitted previously by anybody for the award of any Degree or Diploma to any other University. We also declare that any Intellectual Property Rights generated out of this project carried out at MVJCE will be the property of MVJ College of Engineering, Bengaluru and we will be one of the authors of the same.

Place: Bengaluru

Date: 13 August 2022

Name Signature

1. ADITYA S (1MJ19AS003)

2. KIRAN KB (1MJ19AS020)

3. PAWAR VAIBHAV BHUPENDRA (1MJ19AS029)

4. SATHVIK SWAMY (1MJ19AS039)

ACKNOWLEDGEMENT

The satisfaction and euphoria that accompany a successful completion of task would be incomplete without mention of people who made it possible. So, with gratitude we acknowledge all those who have guided and encouraged us as a beacon of light and crowned my effort with success.

We take this opportunity to convey our gratitude to the **Management of MVJ College of Engineering**, Bengaluru for providing excellent facilities and academic ambience making us feel proud to be a part of this esteemed Institution.

We are extremely happy to submit our sincere thanks to **Dr. P. Mahabaleswarappa**, Principal, MVJ College of Engineering, Bengaluru, for being a constant inspiration and providing all the facilities that was needed throughout the mini project work.

We like to express our gratitude to **Dr. M Brindha** Vice Principal, MVJ College of Engineering, Bengaluru, for the constant encouragement throughout the course.

We like to express our gratitude to **Dr. M. A Lourdu Anthony Raj**, Controller of Examinations, MVJ College of Engineering, Bengaluru, for the guidance & suggestions to complete the mini project work.

We are thankful to **Prof. S C Gupta,** Head of Aerospace Department, MVJ College of Engineering, Bengaluru, for his valuable support and guidance in completing the mini project.

We express, sincere and grateful credit to our guide, Department of Aerospace Engineering, MVJ College of Engineering, Bengaluru, for his constant support and guidance. His valuable suggestion & constant motivation helped us to successfully complete our mini project.

We would like to thank, all Professors and staffs at the Department of Aerospace Engineering, MVJ College of Engineering, Bengaluru for their kind help and co-operation throughout the course.

We sincerely thank our parents, friends, and seniors for giving us the moral support for successful completion of the mini project work.

1. ADITYA S (1MJ19AS003)
2. KIRAN KB (1MJ19AS020)
3. PAWAR VAIBHAV BHUPENDRA (1MJ19AS029)
4. SATHVIK SWAMY (1MJ19AS039)

ABSTRACT

Telescopes and Satellites that are sent to space have many sensitive instruments like photon receptors, camera lens, near-infrared spectrograph (NIRSpec) etc. These instruments require a specific temperature to function and hence the use of a heat shield becomes a necessity. Satellites require heat shields larger than can be accommodated either within the launch vehicle fairing, or within acceptable payload volumes, so deployable shields are the only possible option. A recent example of a deployable heat shield was seen in the James Webb space telescope which was launched in December 2021. A major requirement for designing a heat shield deployment system is that the folded structure should deploy in a smooth manner and that the process of deployment should be a simple one. Our design of the heat shield deployment system achieves the goal of having less points of failure and a simple opening and closing mechanism.

We have designed a folding square frame which uses a lead screw placed at its diagonal for opening and closing operations. A combination of bevel gears is used such that the adjacent arms of the square frame can unfold at right angles. The parts of the square frame are designed in Solidworks software and 3D printer is used for the fabrication of these parts. After the fabrication of all the parts, the frame is assembled and is fixed on top of a lead screw. A motor is fixed to the lead screw using a shaft coupler. Lead screw converts the rotational motion of the motor into linear motion.

The square frame design for the heat shield deployment system is an efficient design as the deployed structure covers approximately twenty-three times more area than the folded structure. The energy consumption is less as only one motor is used in the entire deployment process. In case of detection of any prospective points of failure, easy corrective measures can also be taken because of the simple design.

ACRONYMS

Acronym	Abbreviation
USN	University Seat Number
SEM	Semester
BC	Boundary Conditions
JSWT	James Webb Space Telescope
ACME	American Corps of Mechanical Engineering
PLA	Poly Lactic Acid
PP	Polypropylene
PE	Polyethylene
PS	Polystyrene
NIRcam	Near Infrared Camera
NIRSpec	Near Infrared Spectroscopy
FGS	Fine Guidance Sensor
NIRISS	Near Infrared Imager and Slit less Spectrograph
MIRI	Mid-Infrared Instrument
i.e	That is,
3D	Three Dimensional
LM guide	Linear Motion Guide
DAK	Double Aluminized Kapton
NASA	National Aeronautics and Space Administration
℃	Celsius
°F	Fahrenheit
W	Watt
m	meter
mm	Milli meter

g	Grams
Cm	Centimeter
Mpa	Megapascals
J	Joules
P_R	Force on body by the lead screw
f	Friction Force
F	Weight of the structure
d_m	Mean Diameter
l	Length
F_x	Force component in horizontal direction
F_y	Force component in Vertical direction
N	Normal Force
N	Newton
λ	Angle of twist
T	Torque
T_R	Torque in clockwise direction
T_L	Torque in anti-clockwise direction
A	Ampere
V	Volts
P	Force
D	Diameter

TABLE OF CONTENTS

List of Figures

List of Tables

CHAPTER-1

INTRODUCTION

Introduction

Heat shields are structures that provide protection to a component or a person. Heat shields are applicable in many fields like satellites, re-entry vehicles, car engines, telescopes, etc. Our project will focus on the heat shields used in space. The sun-shield separates the space observatory into a warm, sun facing side and a cold side where most of the instruments and devices reside. This way the sun-shield protects the telescope from external sources of light and heat. The main problem that arises when sending such a giant structure to space in a rocket is to design the structure in such a way that it can be accommodated inside the limited space of a rocket payload. This project deals with this issue by developing a new folding mechanism in which the heat shield can fold and properly placed inside the rocket and after the satellite is in orbit the heat shield is able to deploy itself and protect the components which are placed behind it.

1.1 The James Webb space telescope sun-shield

The James Webb Space Telescope will observe primarily the infrared light from faint and very distant objects. In order to detect those faint heat signals, the telescope itself must be kept extremely cold. To protect the telescope from external sources of light and heat (like the Sun, Earth, and Moon) as well as from heat emitted by the observatory itself, Webb has a 5-layer, tennis court-sized sun-shield that acts like a parasol providing shade. [Actual dimensions: 21.197 m x 14.162 m (69.5 ft x 46.5 ft)]

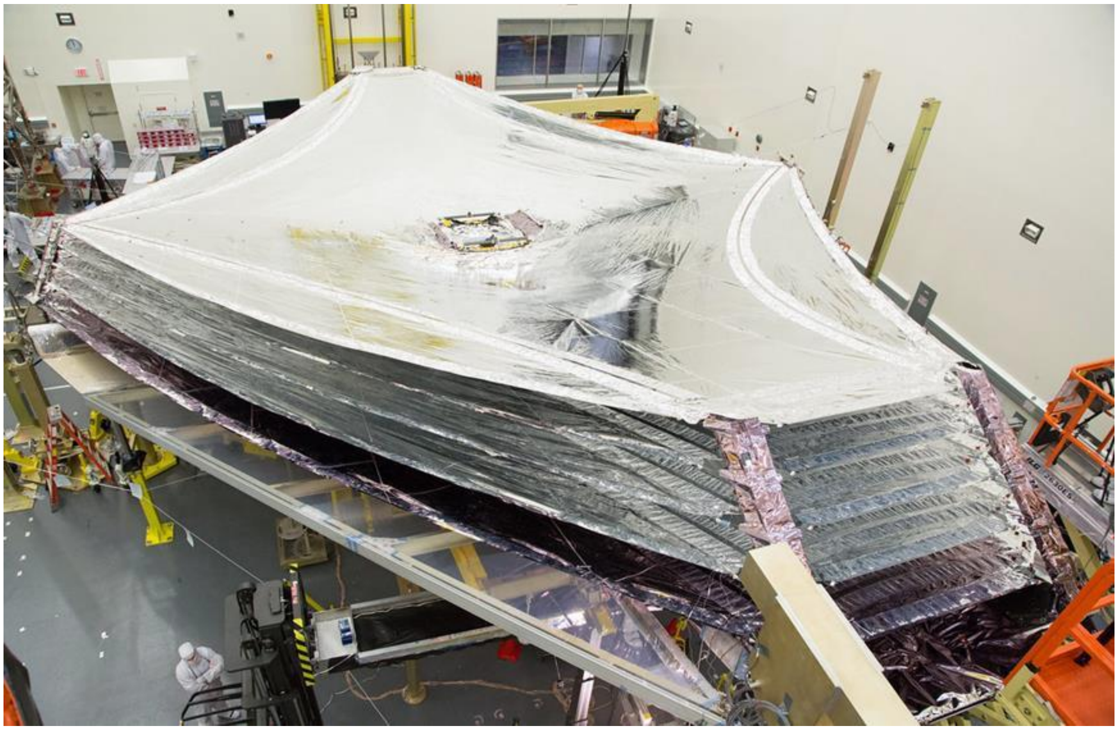

Fig. 1.1 The five-layer heat shield for the James Webb space

This sun-shield will always be between the Sun/Earth/Moon and the telescope. It's able to be positioned this way because JWST will be orbiting the Sun 1.5 million kilometres away from (but approximately in line with) the Earth.

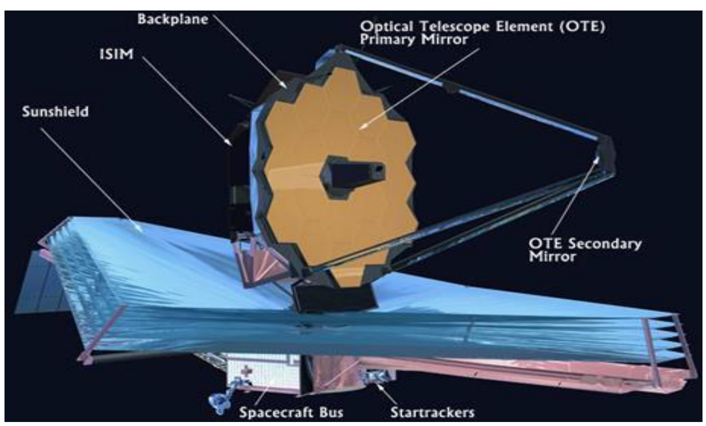

Fig. 1.2 Location of sun-shield on the James Webb telescope

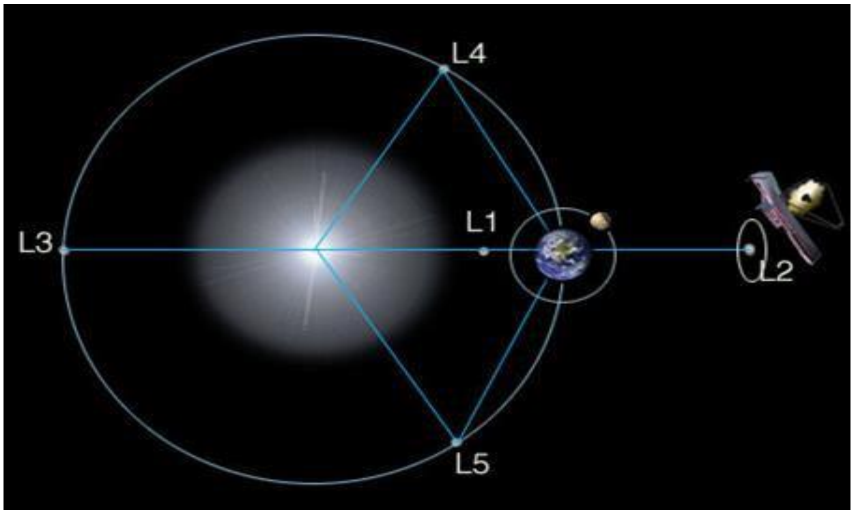

Fig. 1.3 Position of JWST relative to Sun

The sun-shield will allow the telescope to cool down to a temperature below 50 Kelvin (-370°F, or -223°C) by passively radiating its heat into space. The near-infrared instruments (NIRCam, NIRSpec, FGS/NIRISS) will work at about 39 K (-389°F, -234°C) through a passive cooling system. The mid-infrared instrument (MIRI) will work at a temperature of 7 K (-447°F, -266°C), using a helium refrigerator, or cryocooler system.

In addition to providing a cold environment, the sun-shield provides a thermally stable environment. This is essential to maintaining proper alignment of the primary mirror segments as the telescope changes its orientation to the Sun.

Why does the sunshield have five layers instead of just a single thick one? Each successive layer of the sunshield is cooler than the one below. The heat radiates out from between the layers, and the vacuum between the layers is a very good insulator. One big thick sunshield would conduct the heat from the bottom to the top more than five layers separated by vacuum.

Each layer is made from a unique composite material, each has a specific thickness and size, and they must be precisely separated in space. There are even special seams and reinforcements to limit meteorite damage. The sunshield layers are also coated with aluminium and doped-silicon for their optical properties and longevity in the space environment. Doping is a process where a small amount of another material is mixed in during the Silicon coating process so that the coating is electrically conductive. The coating needs to be electrically conductive so that the Membranes can be electrically grounded to the rest of JWST and will not build up a static electric charge across their surface. Silicon has a high emissivity, which means it emits the most heat and light and acts to block the sun's heat from reaching the infrared instruments that will be located underneath it. The highly-reflective aluminium surfaces also bounce the remaining energy out of the gaps at the sunshield layer's edges.

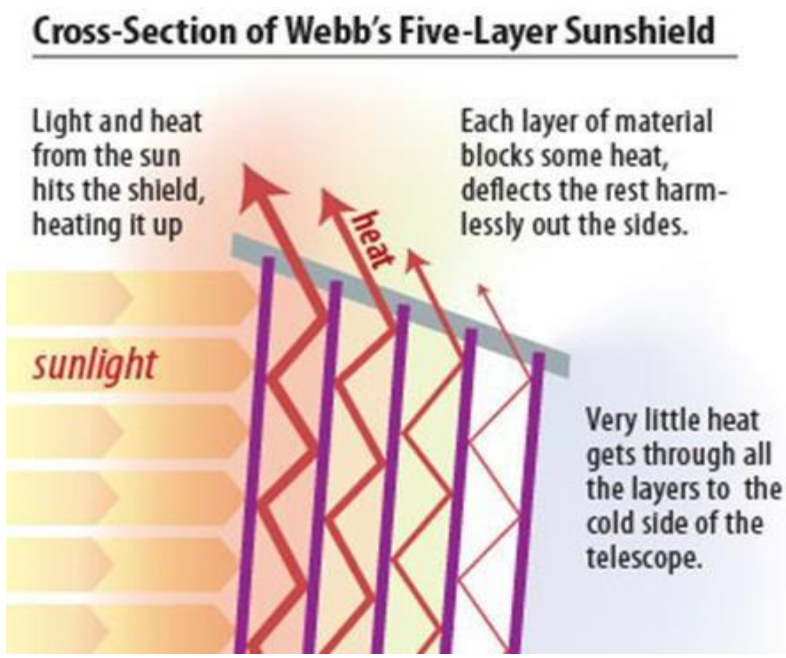

Fig. 1.4 Cross section of the five-layer sunshield

The sunshield is a critical part of the Webb telescope because the infrared cameras and instruments aboard must be kept very cold and out of the sun's heat and light to function properly.

1.2 Alternate uses of a deployment system

1.2.1 Star-shade

Astronomers have been indirectly detecting exoplanets for more than 15 years but taking a picture of one has proven an immensely difficult task. Picking out the dim light of a planet from a star billions of times brighter is akin to finding a needle in a cosmic haystack, especially when the planet in question is a small, rocky world like Earth. In order to achieve this feat, researchers are developing techniques to block out the starlight while preserving the light emitted by the planet. This is called starlight suppression.

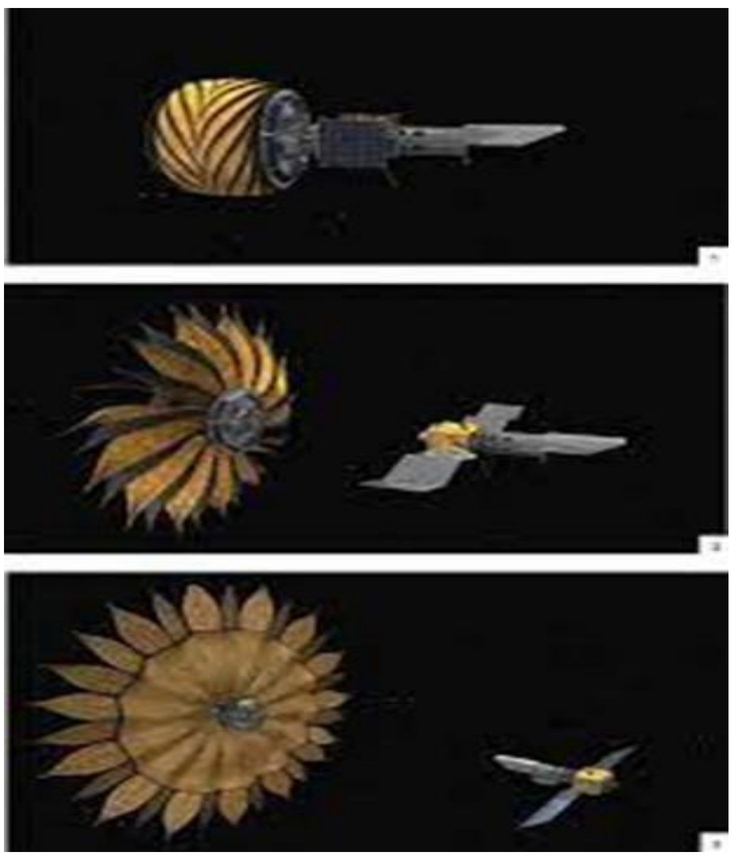

Fig. 1.2.1 (a) Star-Shade Opening

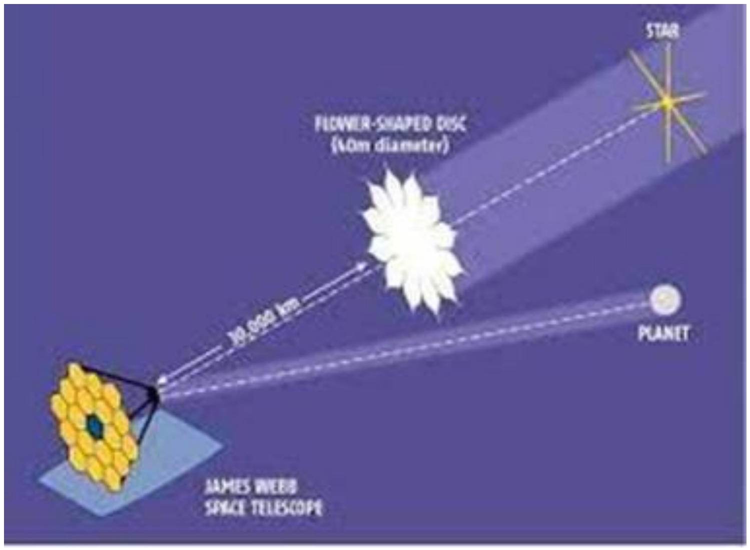

Fig. 1.2.1 (b) Star-Shade Position

It's a task that NASA's flower-shaped star-shade is designed to make easier. Working in conjunction with a space-based telescope, the star-shade can position itself precisely between the telescope and the star that's being observed and can block the starlight before it even reaches the telescope's mirrors.

With the starlight suppressed, light coming from exoplanets orbiting the star would be visible. Using this technology, astronomers would be able to take actual pictures of exoplanets – images that could provide clues as to whether such worlds could support life as we know it.

1.2.2 Solar sails

Solar sailing is a revolutionary way of propelling a spacecraft through space.

A solar sail spacecraft has large reflective sails that capture the momentum of light from the Sun and uses that momentum to push the spacecraft forward

Light is made up of particles called photons. Photons don't have any mass, but as they travel through space, they do have momentum. When light hits a solar sail which has a bright, mirror-like surface the photons in that light bounce off the sail (i.e., they reflect off it, just like a mirror). As the photons hit the sail their momentum is transferred to it, giving it a small push. As they bounce off the sail, the photons give it another small push. Both pushes are very slight, but in the vacuum of space where there is nothing to slow down the sail, each push changes the sail's speed.

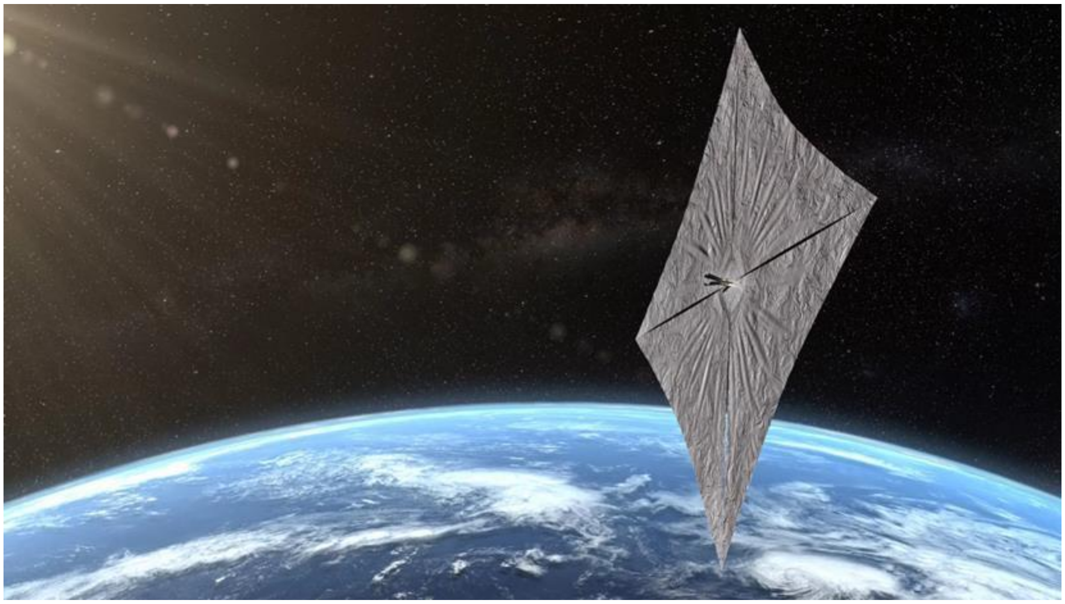

Fig. 1.2.2 Solar Sail

Spacecraft gain most of their momentum when they are launched from Earth, and then most increase their speed or change course using chemical rockets that burn fuel that the spacecraft carries on board. But more rocket fuel means more weight, which limits how much can be carried. Most spacecraft reach their maximum speed and then coast through space or rely on gravity assists from other planets to reach their destinations.

With solar sails, a spacecraft can continue accelerating as long as there is light pushing on it. Within a solar system, sunlight can continuously push on the sail, accelerating the spacecraft throughout its entire voyage. This means that solar sail-propelled spacecraft can reach speeds that would be practically impossible for chemical rockets to achieve.

Solar sailing spacecraft are also advantageous because they can be placed in orbits that would otherwise be unstable by using the sail acceleration as a balancing force. As an example, this could enable solar monitoring missions to sit between the Earth and Sun at a closer distance than otherwise possible to provide more warning of solar storms.

1.3 Methodology used for making the Heat Shield deployment system

The project began with the selection of a square shaped folding design. The idea was to use a linear actuator for unfolding the closed heat shield. The linear actuator used in this project is a lead screw. The lead screw dimensions were first determined based on need and budget restrictions. Then on the base of lead screw dimensions the dimensions of the frame and its parts was calculated. Once we found all the required dimensions the parts were designed in solid-works and were fabricated using a 3D printer. He 3D printed parts of the frame were assembled and the opening and closing operations were checked.

A base plate was made on which the lead screw and the motor were fixed. The motor was connected to the lead screw using a shaft coupler.

The complete frame was placed on the lead screw and the opening and closing mechanism was again checked. The motor turns the leadscrew through the shaft coupler and the lead screw converts this rotational motion into linear motion. The end of the frame attached to the lead screw nut moves linearly along with the lead screw nut resulting in the opening of the folded mechanism.

CHAPTER-2

Literature survey

Literature survey

2.1) Linear Actuators

Ball screws are often viewed as the first choice for linear motion applications because the use of recirculating ball bearings provides a high level of efficiency, load capacity and positioning accuracy. However, with careful attention to selection and application, lead screws can deliver efficiency that comes close to ball screws on many applications, high levels of load capacity and very good positioning accuracy.

Lead screws also offer many other advantages such as more flexible configuration and form factor, the ability to operate without lubricant, quieter operation, clean materials, and lower cost. Here we will discuss how to determine whether a particular application is a good fit for lead screws, and how to select the right lead screw for the application.

Lead screws use the helix angle of the thread to convert rotary motion to linear motion. The performance of a lead screw is heavily dependent on the coefficient of friction between the nut and the screw, which in turn depends upon the material used for the nut and screw. Lead screws typically use nuts made of internally lubricated plastic or bearing-grade bronze. Plastic nuts usually travel on stainless steel screws while bronze nuts often run-on carbon steel screws. When bearing-grade bronze nuts are used, stainless steel screws are an option.

Load capacity in considering whether lead screws or ball screws are the best for an application, begin by looking at the required load capacity. Plastic nuts are typically used for light loads of less than 100 pounds, although plastic nut designs for 300 pounds and beyond are possible. Bronze nuts, on the other hand, can be used for applications in excess of several thousand pounds. Ball screws generally provide equal or better load capacity than lead screws, so they are a better choice if the load requirements exceed lead screw capabilities.

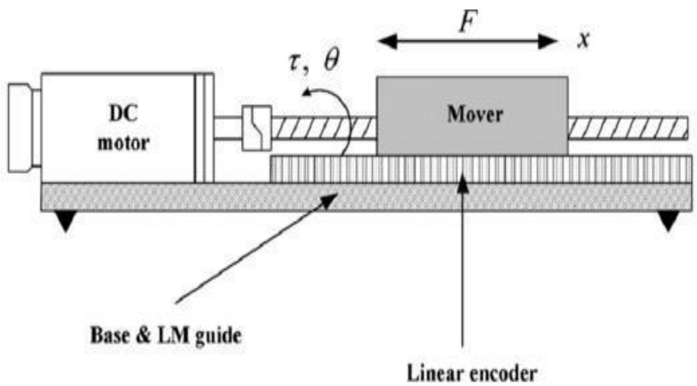

Fig. 2.1 Lead Screw mechanism

As a general rule, higher helix angles mean higher efficiency. A higher helix angle is more efficient because less of the energy used to drive the lead screw goes into overcoming friction. This is because the number of times the screw must rotate to achieve the same linear displacement is reduced on a high helix screw. A disadvantage of a high helix angle is that more torque is required to turn the screw.

Conclusion: Lead screws provide a versatile and economical linear motion solution. Lead screws have relatively straight-forward geometry and performance and offer the flexibility to be adapted to the needs of most applications. While there are many applications that require the high stiffness, thrust capacity and absolute accuracy of ball screws, in many cases lead screws can be engineered to meet performance requirements and provide advantages over a ball screw at a substantially lower cost.

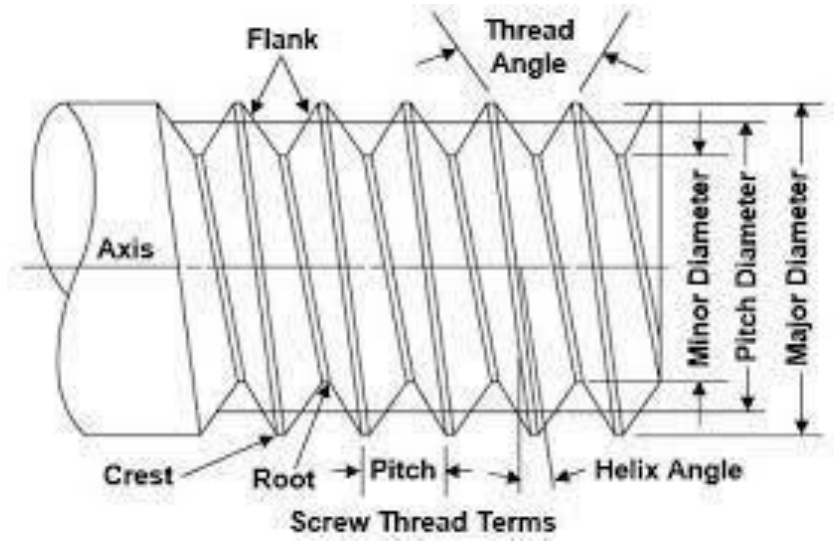

Fig. 2.2 Threading

<u>Type of thread used</u>

<u>ACME thread</u>

Trapezoidal thread forms are screw thread profiles with trapezoidal outlines. They are the most common forms used for leadscrews (power screws). They offer high strength and ease of manufacture. They are typically found where large loads are required, as in a vice or the leadscrew of a lathe. Standardized variations include multiple-start threads, left-hand threads, and self-centring threads (which are less likely to bind under lateral forces)

We used this lead screw as it is the most cost effective and widely available lead screw.

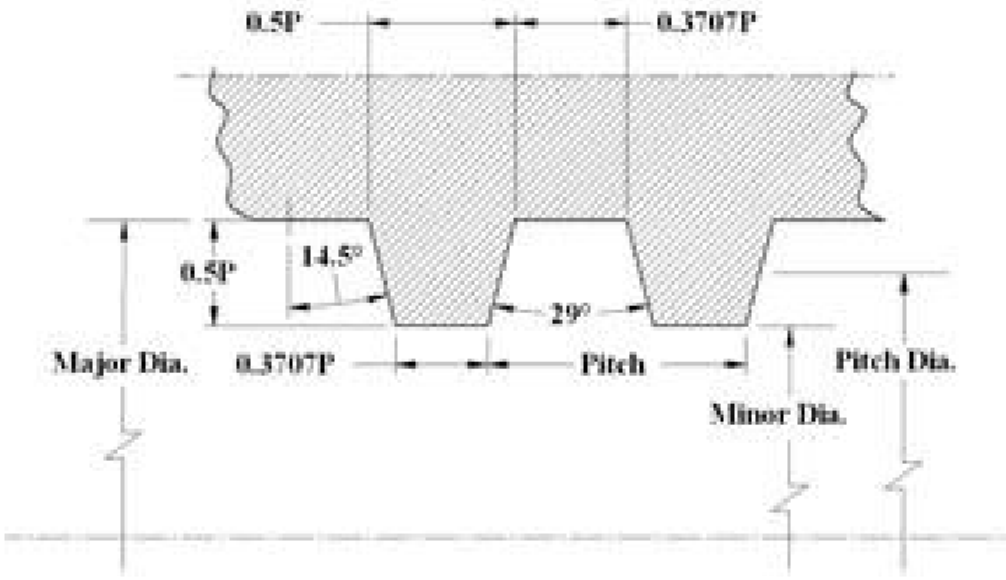

Fig. 2.3 ACME Thread

Lead screw specifications

Thread type	Acme trapezoidal
Rod length	1000 mm
Pitch	2 Mm
Rod material	Stainless steel
Thread angle	29°
Lead	2mm
Outer diameter	8mm

Table 2.1 Lead Screw Specifications

2.2) Double Aluminized Kapton

Kapton polyimide film possesses a unique combination of properties that make it ideal for a variety of applications in many different industries. The ability of Kapton to maintain its excellent physical, electrical, and mechanical properties over a wide temperature range has opened new design and application areas to plastic films. Kapton is synthesized by polymerizing an aromatic dianhydride and an aromatic diamine. It has excellent chemical resistance; there are no known organic solvents for the film. Kapton is self-extinguishing as it has the highest UL-94 flammability rating: V-0. The outstanding properties of Kapton permit it to be used at both high and low temperature extremes where other organic polymeric materials would not be functional. Adhesives are available for bonding Kapton to itself and to metals, various paper types, and other films.

Double-aluminized Kapton (DAK) is commonly used in multi-layer insulation blankets in cryogenic systems. NASA plans to use individual DAK sheets in lightweight deployable shields for satellites carrying instruments. A set of these shields will reflect away thermal radiation from the sun, the earth, and the instrument's warm side and allow the instrument's cold side to radiate its own heat to deep space. In order to optimally design such a shield system, it is important to understand the thermal characteristics of DAK down to low temperatures. We describe experiments which measured the thermal conductivity and electrical resistivity down to 4 Kelvin and the emissivity down to 10 Kelvin

Amongst the 3 modes of heat transfer conduction and radiation are the only 2 possible modes of heat transfer since convection is not possible in space due to the absence of atmosphere. The low thermal conductivity of Kapton allows the heat shield to minimize conduction as much as possible, so therefor, the heat transferred to the other side of the heat shield would be less. Radiation can be minimized by coating the Kapton material with aluminium.

Kapton has been used successfully in applications at temperatures as low as -269°C (-452°F) and as high as 400°C (752°F). This makes it a very reliable material in space environment where temperatures fluctuate rapidly. Kapton coated with a thin layer of aluminium makes it possible to reflect majority of the radiation falling on it thus making it safer for the components its protecting.

Properties of Kapton

Thermal conductivity	0.75 W/m·K
Density	1.42 g/cm³
Ultimate tensile strength (thickness 25micro meter)	231 MPa
Specific heat	1.09 J/g K
Poisson's Ratio	0.34

Table 2.2 Properties of Kapton

2.3) Bevel Gears

Bevel gears are gears where the axes of the two shafts intersect and the tooth-bearing faces of the gears themselves are conically shaped. Bevel gears are most often mounted on shafts that are 90 degree apart but can be designed to work at other angles as well. Since the structure we are making requires perpendicular motion, we are making use of bevel gears. For the square frame structure, we require a total of 6 bevel gears. Since there is no need to vary the torque or speed, we require identical gears which can only transfer the motion. Therefore, the calculations of the gear variables have been determined and the gears are selected.

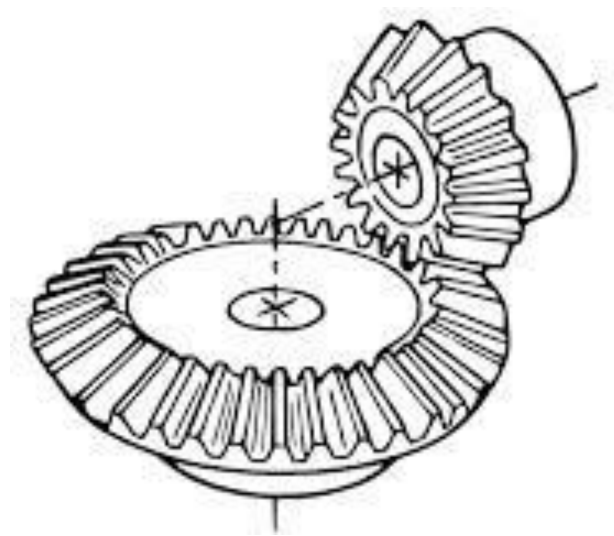

Fig. 2.4 Bevel Gears

2.4) Knuckle joint

A knuckle joint is a mechanical joint used to connect two rods which are under a tensile load, when there is a requirement of small amount of flexibility, or angular moment is necessary. There is always axial or linear line of action of load.

The knuckle joint assembly consists of the following major components:

- Single eye end
- Double eye end or fork
- Knuckle pin.

Our structure makes use of the knuckle joint where there is only 1 degree of freedom. Th fork of the joint is connected to the rod and the single eye end is on the support. The pin holds the single eye and the fork together Few of the advantages of knuckle joint are:

Knuckle joint can withstand large tensile loads.

- It has good mechanical rigidity.
- It is simple to manufacture and set up.
- It can be easily assembled and dismantled.
- Design is simple and easy.
- Cost effective and reliable.
- It can permit angular movement between rods.

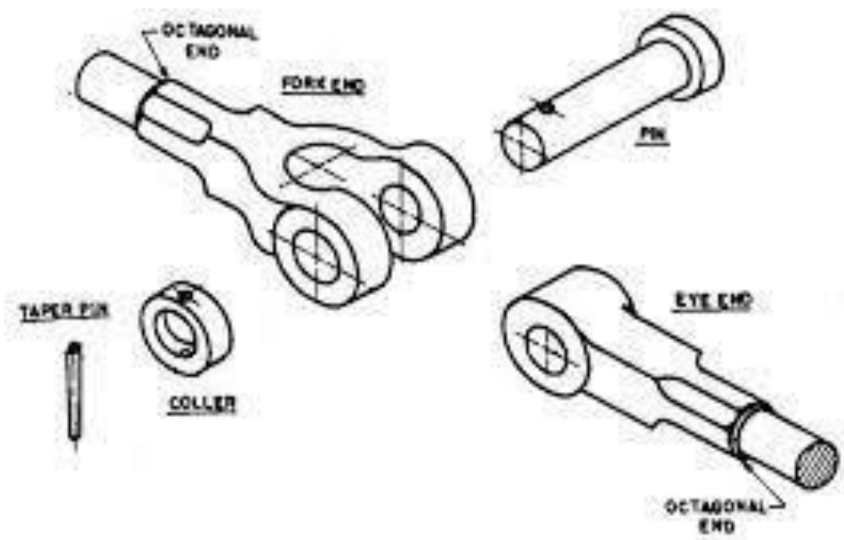

Fig. 2.5 Knuckle Joints

2.5) Aluminium rod

For the frame the main load carrying member will be the rods that connect the 2 joints. We decided to go with hollow aluminium rods. Aluminium provides a good strength to weight ratio which is what we were going for.

The alloy aluminium 6061 containing magnesium and silicon as its major alloying elements. The nominal composition of type 6061 Aluminum is 97.9% Al, 0.6% Si, 1.0%Mg, 0.2%Cr, and 0.28% Cu. The density of 6061 Aluminum alloy is 2.7 g/cm³. Two important factors when considering mechanical properties are yield strength and ultimate strength.

The yield strength describes the maximum amount of stress needed to elastically deform the part in a given loading arrangement (tension, compression, twisting, etc.). The ultimate strength, on the other hand, describes the maximum amount of stress a material can withstand before fracturing (undergoing plastic, or permanent deformation). For static applications, the yield strength is the more important design constraint as per industry standard design practices; however, the ultimate strength can be useful for certain applications that call for it. 6061 aluminum alloy has a yield tensile strength of 276 MPa , and an ultimate tensile strength of 310 MPa .

CHAPTER-3

METHODOLOGY

Methodology

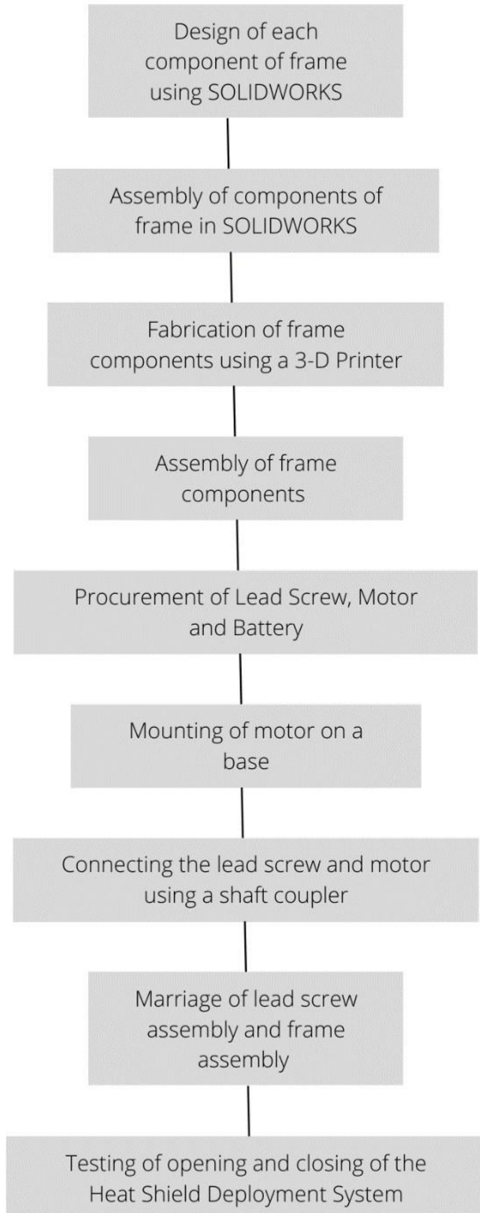

CHAPTER-4

DESIGN OF COMPONENTS

Design Of Components

Each component was designed used SOLIDWORKS based on the required dimensions. The analysis of each component was done on ANSYS WORKBENCH based on the force calculated, the stress on each part was calculated theoretically and compared with the results from ansys.

4.1) <u>Design of Fork</u>

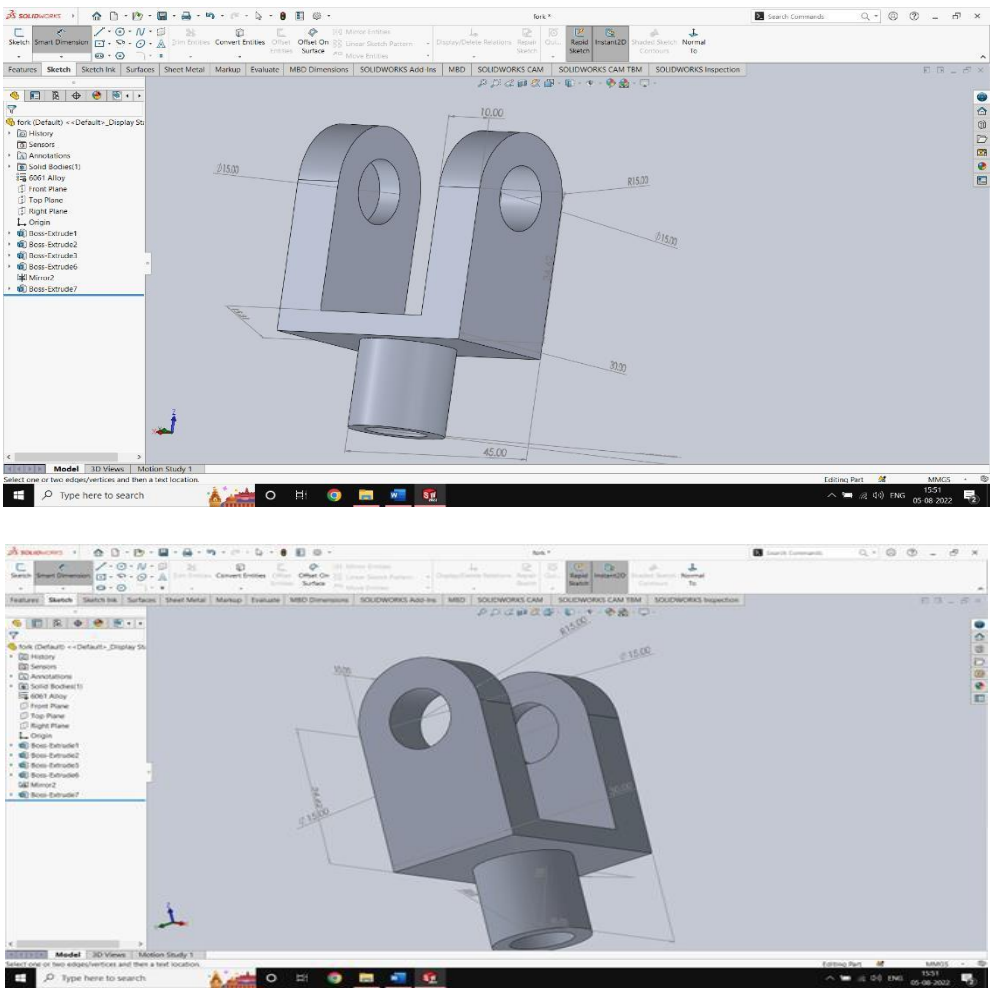

Fig. 4.1 Fork Design

For the design of fork firstly a rectangle of 30mm x 45mm was made and extruded, and then arms were made and extruded. The extrude cut command was used to cut a hole of diameter 15mm. The fillet command was used to curve the edges of the arms. Then at the base 2 concentric circles of diameter 13mm and 20mm were made and using the extrude command was used to extrude 20mm which is where the rod will sit.

4.2) <u>Design of Pin</u>

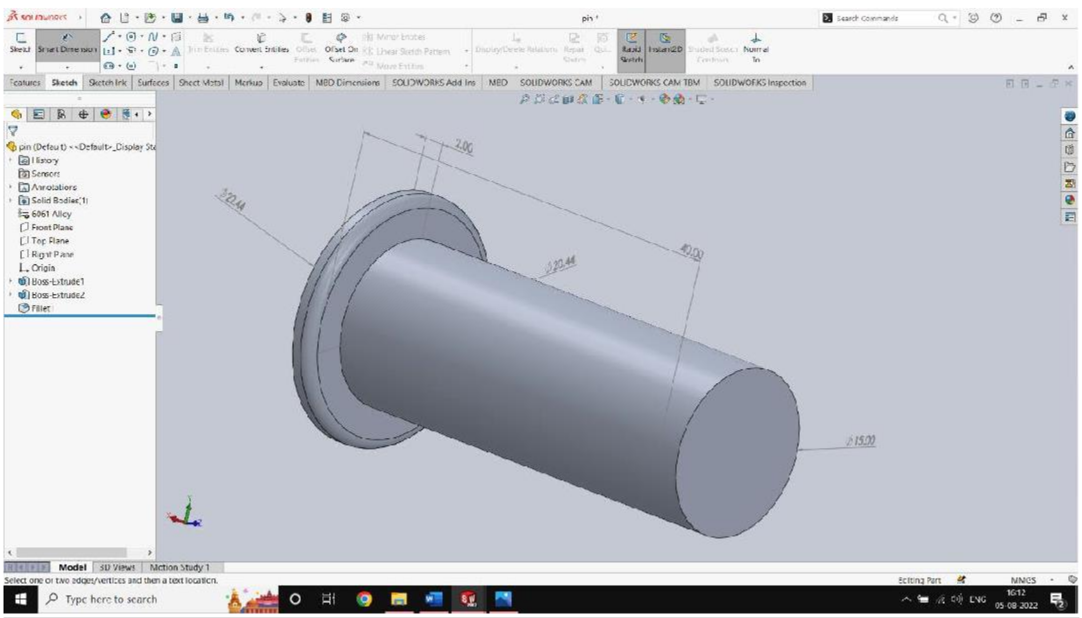

Fig. 4.2 Pin Design

First a sketch plane is taken and a circle of diameter 15mm was made and extrude for a length of 40mm. Then at the surface of the cylinder another sketch plane was taken and a circle of diameter of 22.4mm was taken and extruded to a length of 2mm. Using the fillet command the edges were made blunt.

4.3) Design of L-bracket

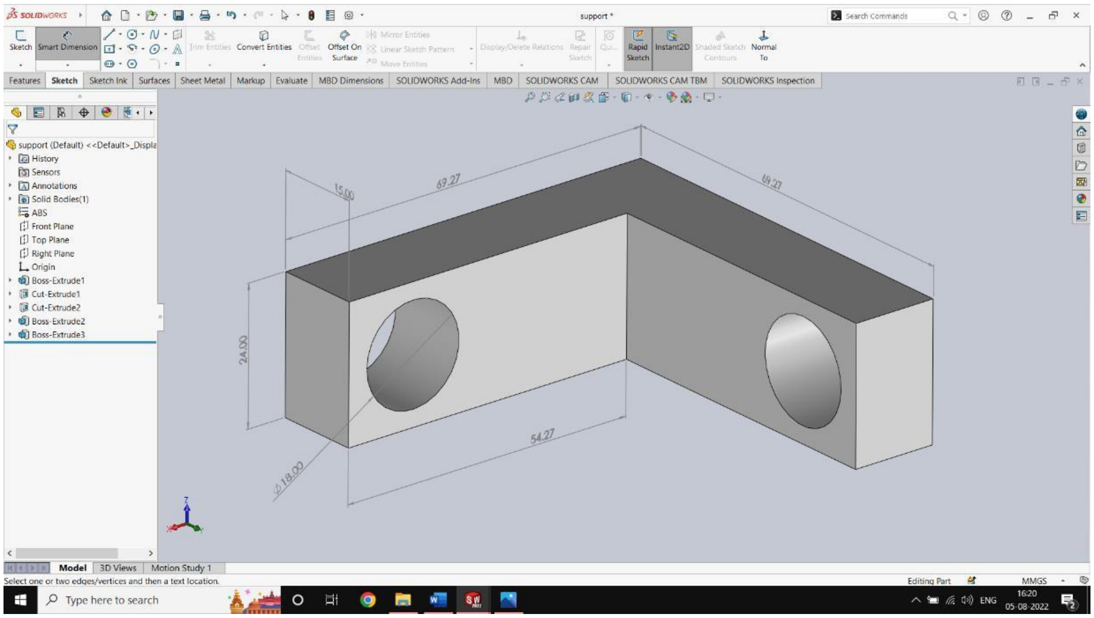

Fig. 4.3 L-Bracket Design

For the L-bracket a new part was taken. A sketch plane was selected. An L shaped sketch of length 69.27mm and thickness 15mm was done. This sketch was extruded to a thickness of 24 mm. At the corner of each arm a circle was made of diameter 18mm and use the command extrude cut the holes were made.

4.4) Design of Bevel Gear

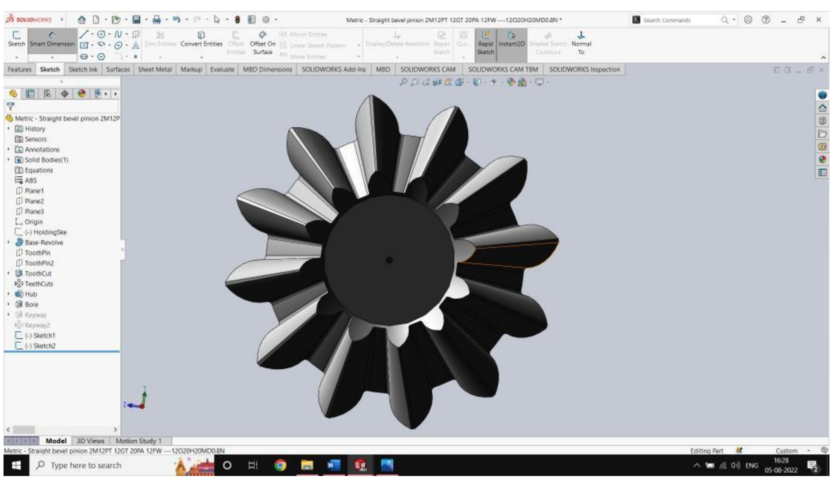

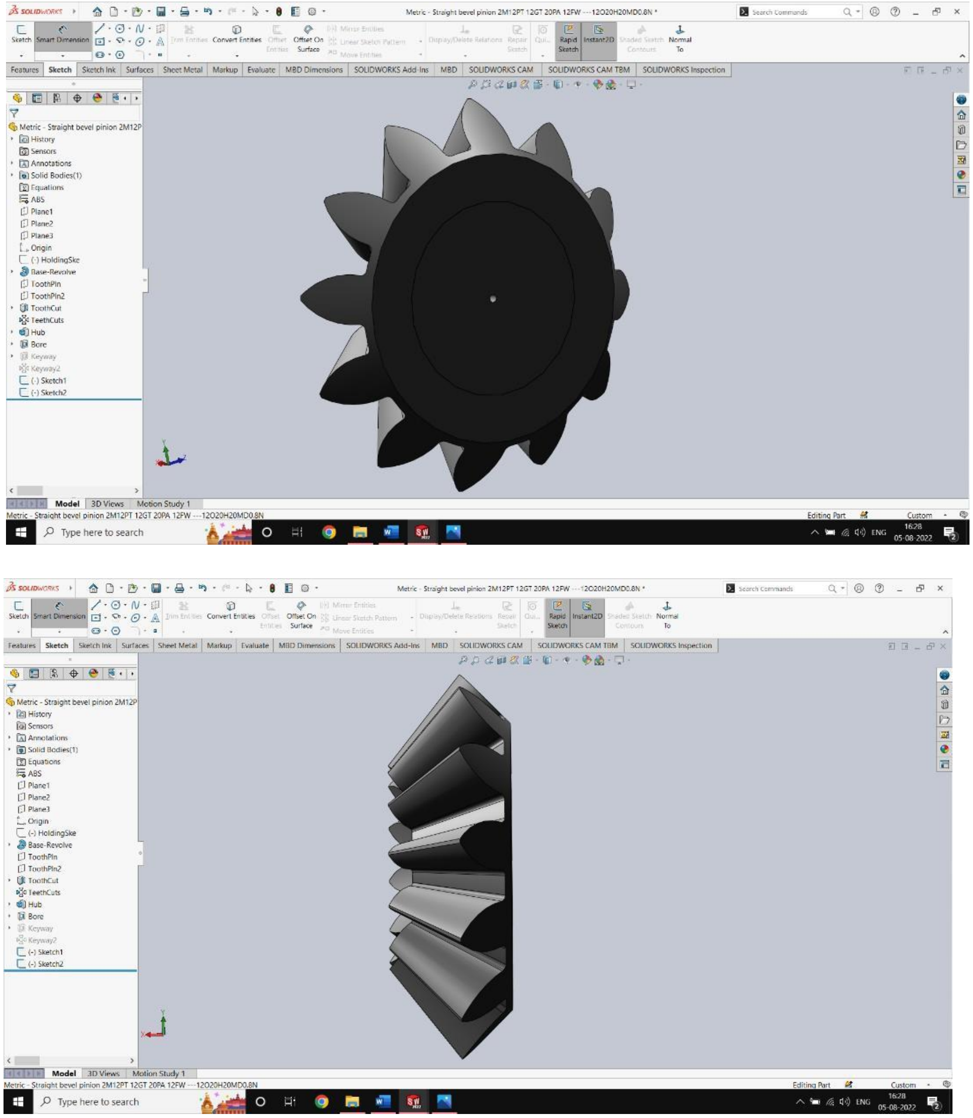

Fig. 4.4 Bevel Gear Design

The modelling of bevel gear was done using standard toolbox from solidwords. The gear was made with the following values:

Module = 3

Number of teeth = 12

Pitch Diameter = 36mm

Pressure Angle = 20°

4.5) Design of Nut

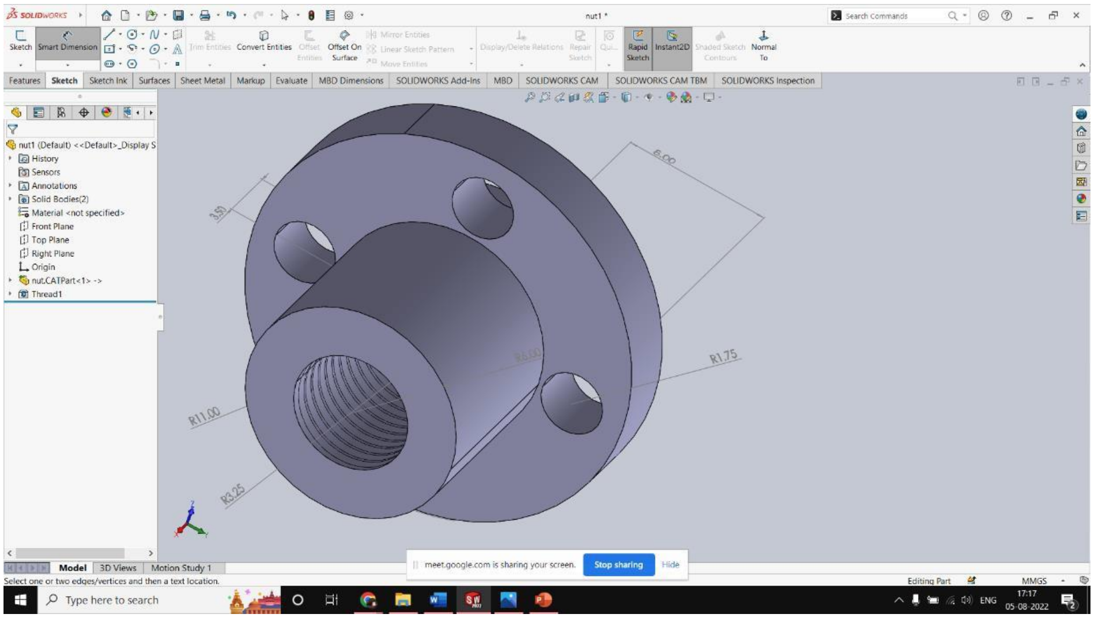

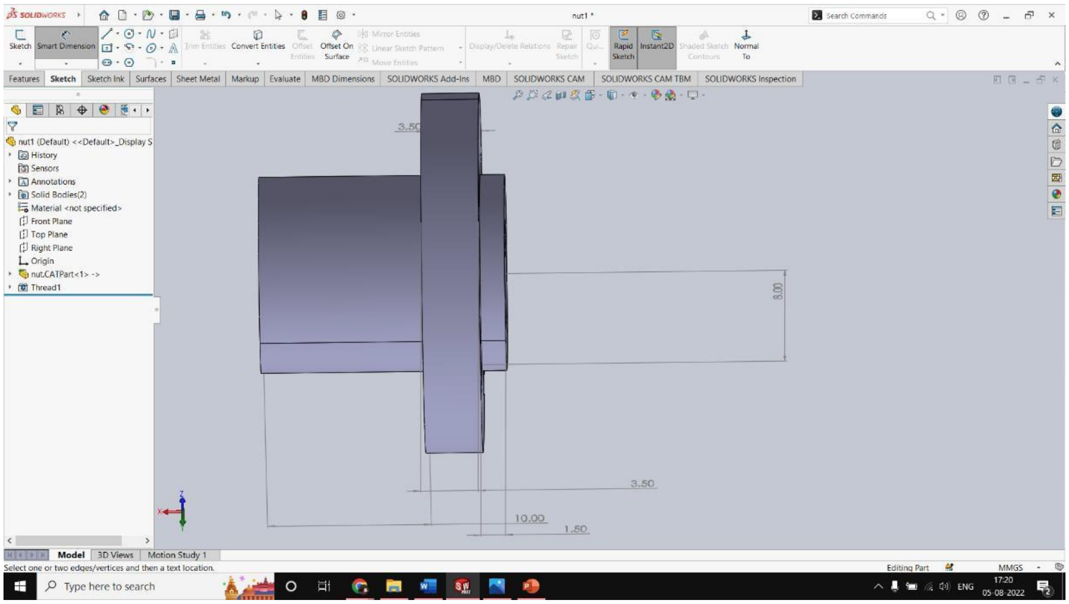

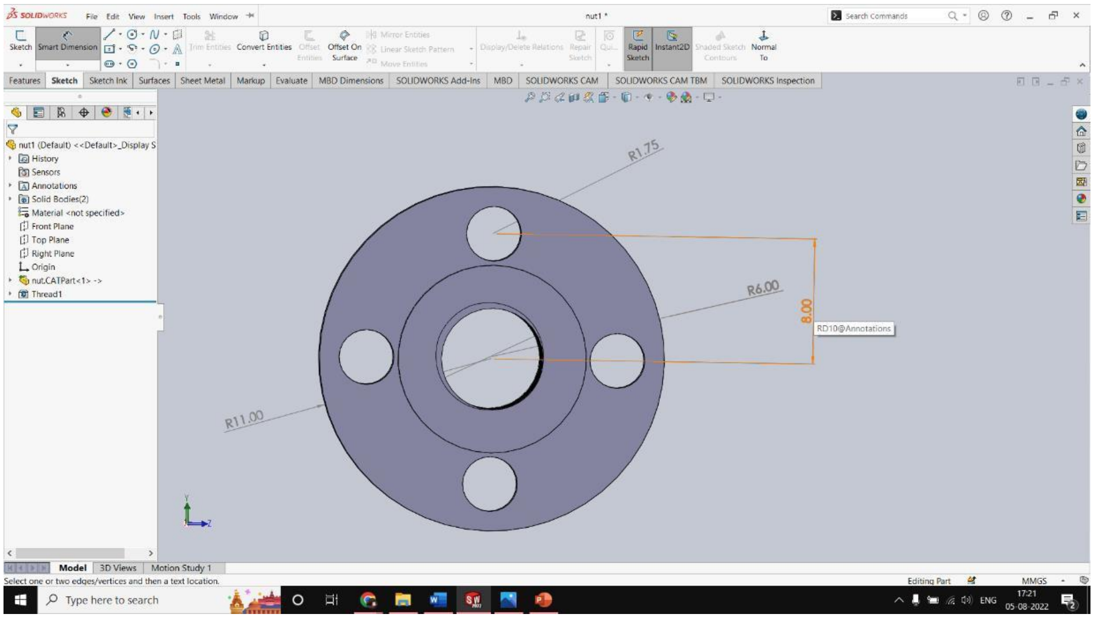

Fig. 4.5 Nut Design

For the modelling of nut, first a plane is selected, a circle or radius 11mm was made and extruded to a thickness of 3.5mm. In the surface of the model a new sketch plane is created and a center circle of radius 8mm and on this circle a circle of radius 1.75mm is made. Using the pattern command 3 more circles are made around the center, and using extrude cut the hole is made. On the same sketch plane 2 concentric circle of radius 6mm and 3.25mm is made, this is extruded to a distance of 10mm. The inner hole is threaded using Hole wizard➔thread command.

4.6) Design of C-cap

There was a problem that arose due to the size of few components because of which another component was designed which could solve this issue. This component was fitted between the fork and the L-bracket. The purpose of the C-cap is to make the joints more rigid.

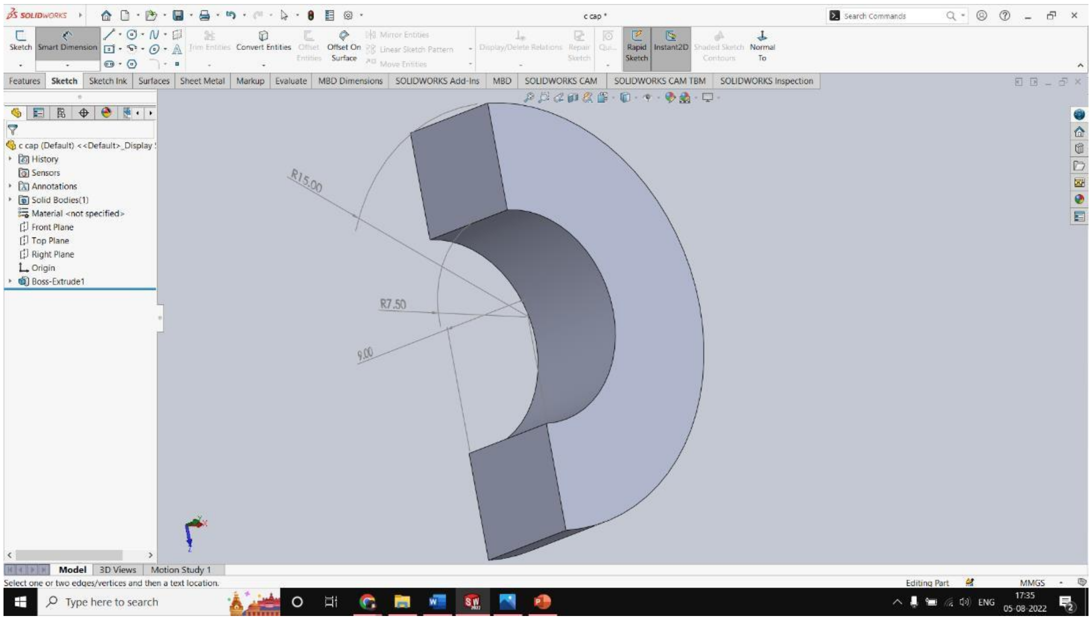

Fig. 4.6 C-Cap Design

For the modelling of C-Cap a sketch plane was selected and a concentric semi-circle of radius 7.5mm and 15mm was made. Both the circles were connected at the ends and this sketch was extruded to a thickness of 9mm.

CHAPTER 5

FABRICATION AND ASSEMBLY

FABRICATION AND ASSEMBLY

5.1) Fabrication

The components of the square frame were fabricated using 3-D printer. 3D printing or additive manufacturing is the construction of a three-dimensional object from a CAD model or a digital 3D model. It can be done in a variety of processes in which material is deposited, joined or solidified under computer control, with material being added together (such as plastics, liquids or powder grains being fused), typically layer by layer.

Traditionally, 3-D printing focused on polymers for printing, due to the ease of manufacturing and handling polymeric materials. The material we decided to go with is PLA plastic (Polylactic acid).

Polylactic acid, also known as PLA, is a thermoplastic monomer derived from renewable, organic sources such as corn starch or sugar cane. Using biomass resources makes PLA production different from most plastics, which are produced using fossil fuels through the distillation and polymerization of petroleum.

Despite the raw material differences, PLA can be produced using the same equipment as petrochemical plastics, making PLA manufacturing processes relatively cost efficient. PLA is the second most produced bioplastic (after thermoplastic starch) and has similar characteristics to polypropylene (PP), polyethylene (PE), or polystyrene (PS), as well as being biodegradable.

The common properties of PLA are mentioned in the given table:

Properties of PLA

PROPERTY	VALUE
Density	1.25 g/cm³
Youngs modulus	4.107GPa
Poisson's ratio	0.3
Tensile yield strength	5.9MPa
Tensile ultimate strength	64MPa

Table 5.1 Properties of PLA

The components that weren3-D printed are as follows: -

- Fork
- Pin
- L-bracket
- Bevel gear
- C-clamps

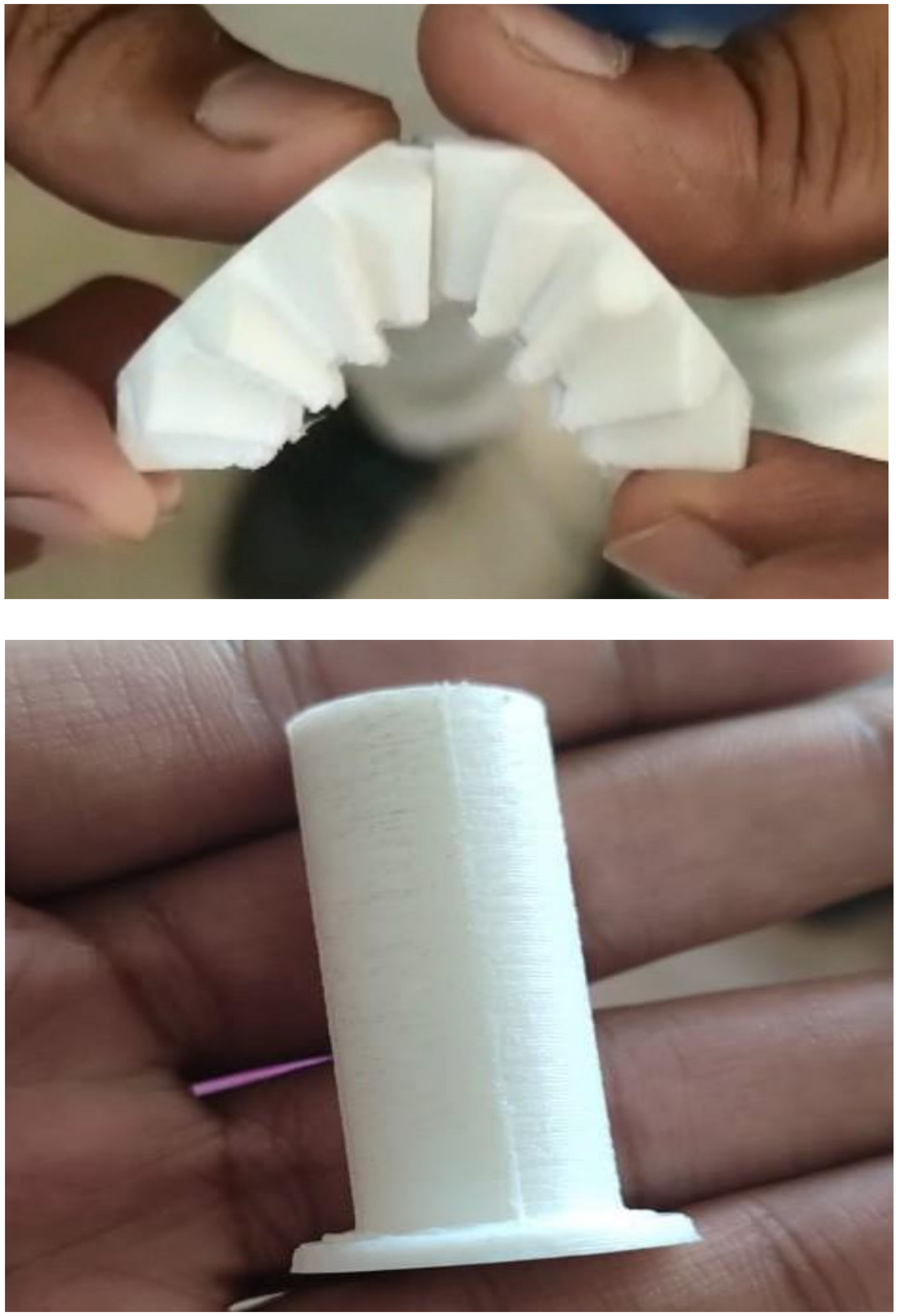

Fig. 5.1 Fabricated Components

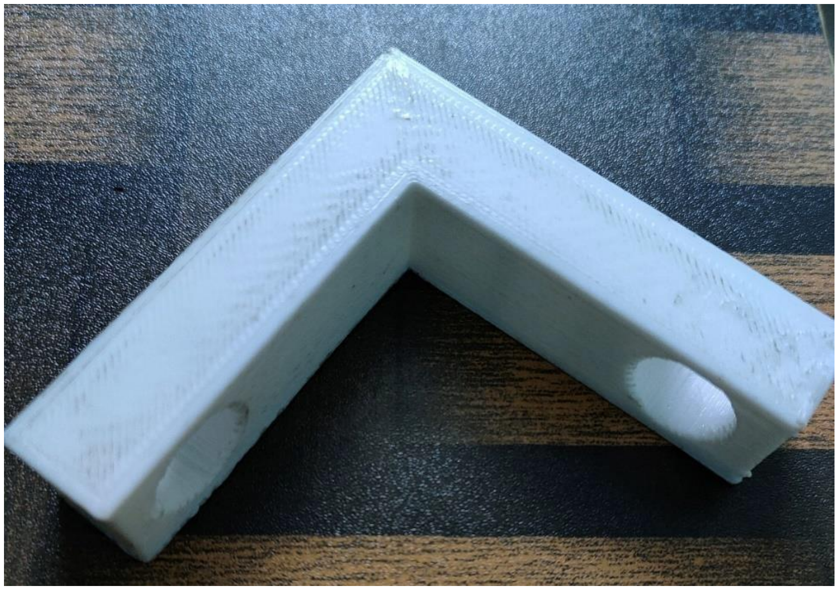

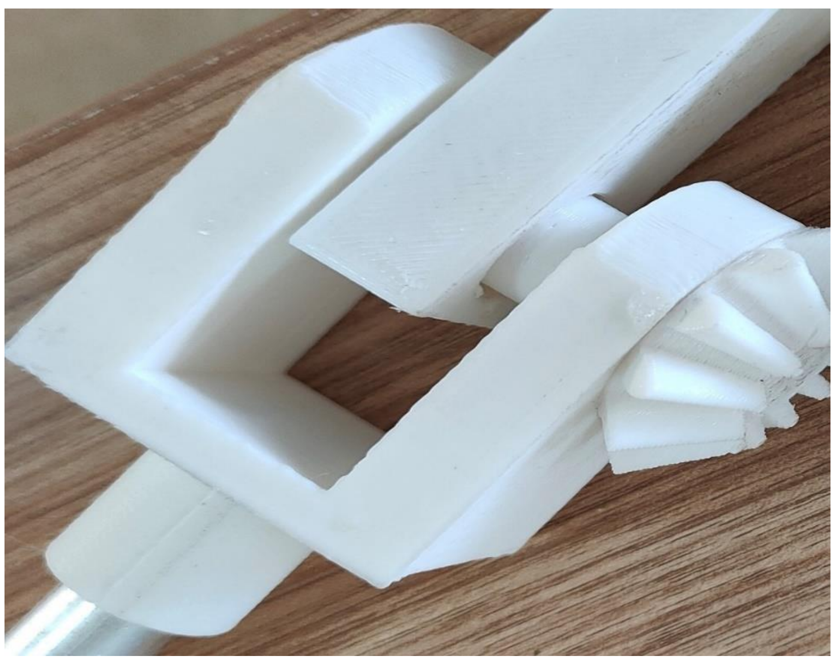

Fig. 5.1 Fabricated Components

5.2) Frame Assembly

After the fabrication of all the components assembly was done. The fork was split in 2 for ease of 3-D printing and the 2parts were later bonded using METLOK 743 adhesive glue.

METLOK 743 Single Component instant bonding Adhesive is an instant adhesive which can used on rubber, wood, plastic, metals. It provides great bonding between the materials with an instant action. It has a strong bond that helps stick a variety of materials.

The same glue was used to fix the bevel gears to the fork, the pin to the inner hole of the fork and the c cap to the pin.

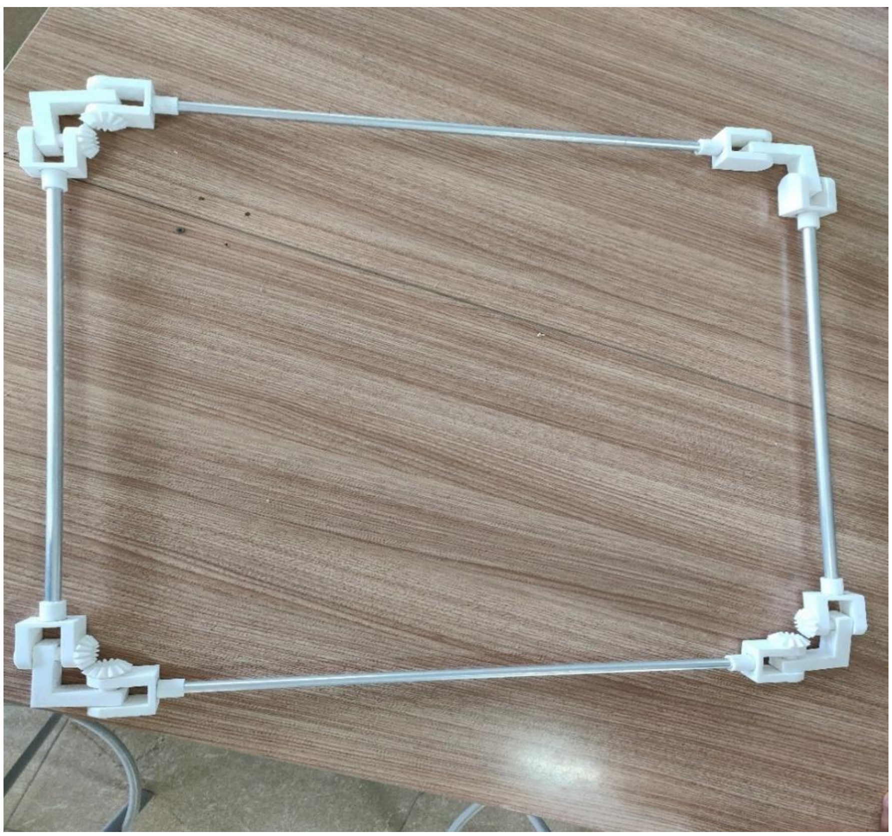

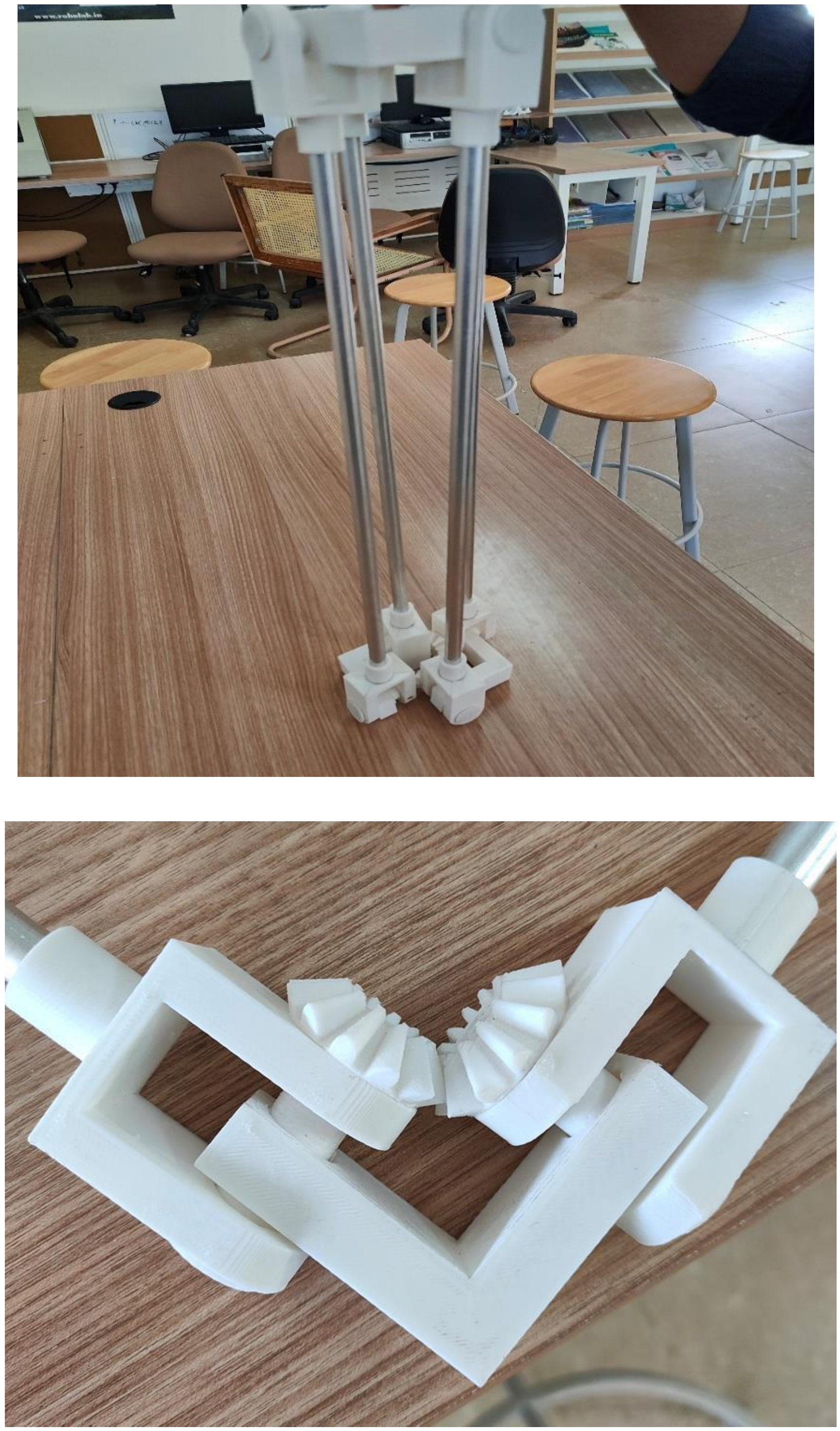

Fig. 5.2 Frame Assembly

5.3) Lead Screw Assembly

The parts of the lead screw assembly are as follows:

- Lead screw
- Shaft coupler
- Motor
- Battery
- Lead screw nut
- Wooden board
- Mount
- Bearings

The motor was fixed to the wooden board using nut and bolt the shaft coupler was used to connect the motor to the lead screw the shaft coupler provides proper transmission of torque from the motor to the lead screw. since our motor shaft had a different diameter than the coupler we had to improvise and use a metal filling to make the connection as rigid as possible

The other end of the shaft coupler was fixed to one end of the lead screw, whereas the other end of the lead screw was fixed using a bearing so that it is free to rotate about one axis.

To power the motor, we soldered wires on the motor and connected to a 12volt battery.

A custom-made mount was designed and placed on top of the motor so that the frame can be fixed. another mount was made on the lead screw nut to fix the other side of the frame. As the lead screw rotates about its axis the nut is made to move linearly along the lead screw, this results in the frame opening and closing.

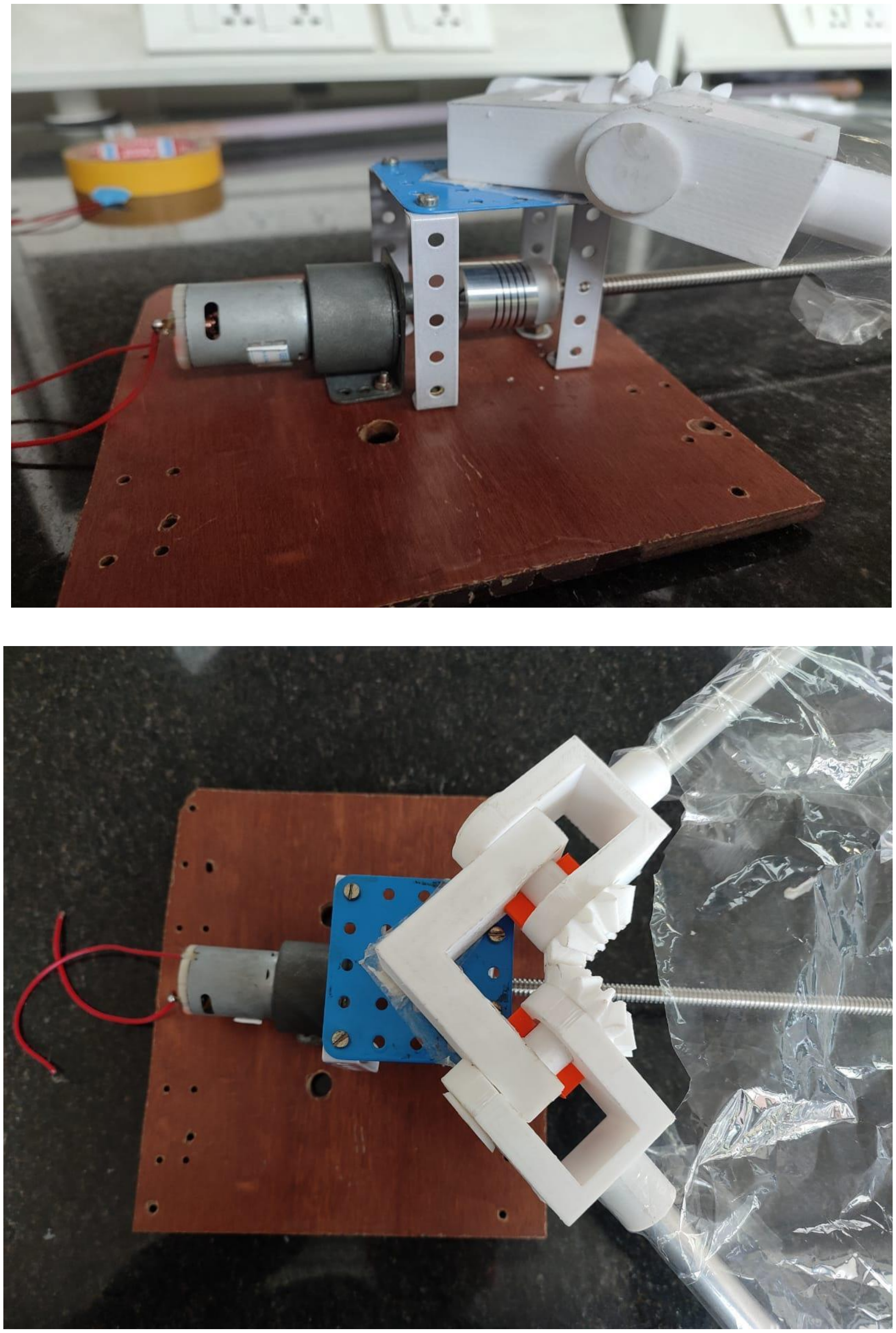

Fig. 5.3 Lead Screw Assembly

5.4) Final Assembly

The frame assembly (Fig 5.2) was fixed on the lead screw assembly (Fig 5.3)

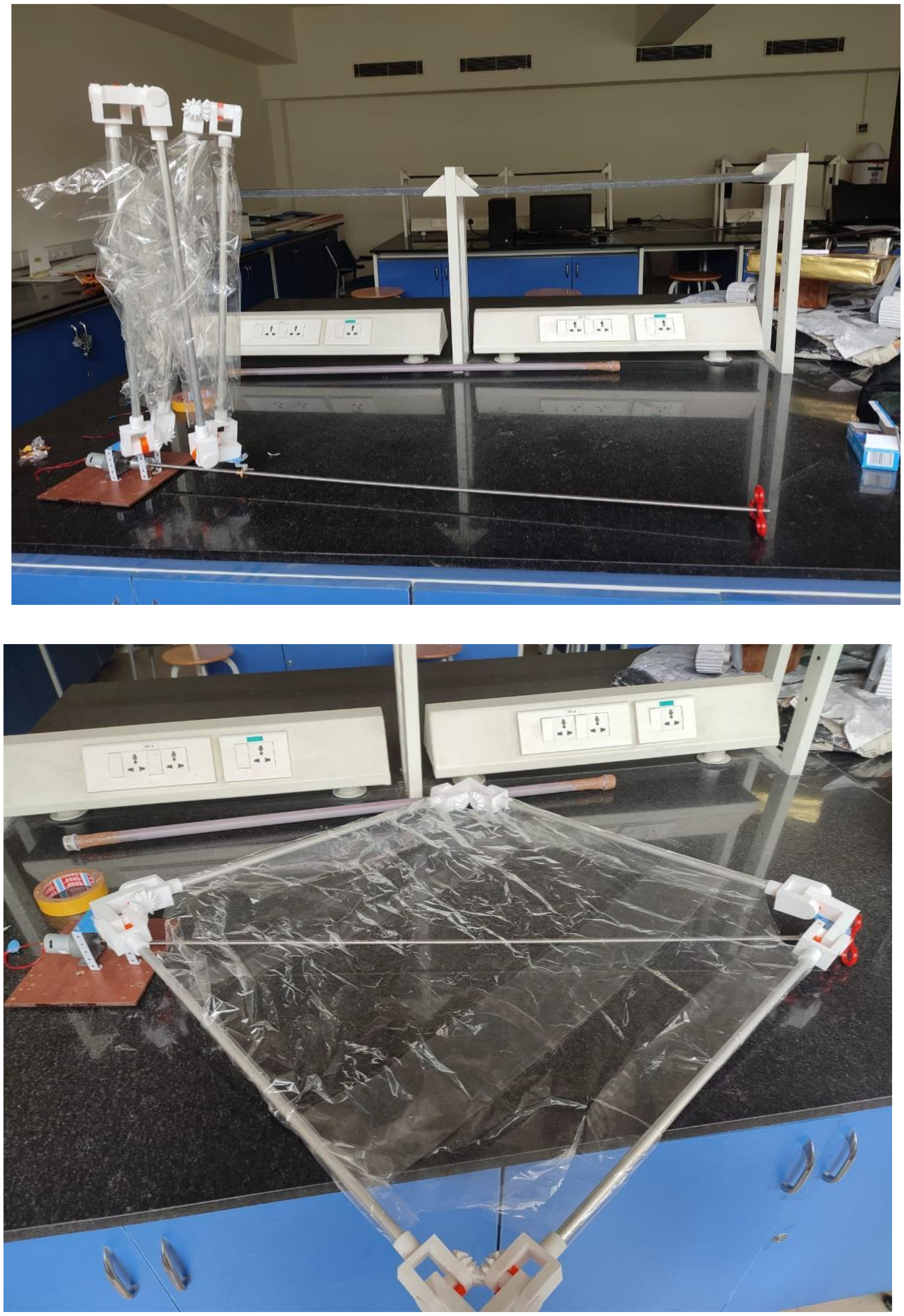

Fig. 5.4 Final Assembly

CHAPTER 6

CALCULATIONS

&

RESULTS

CALCULATIONS & RESULTS

6.1) Calculation

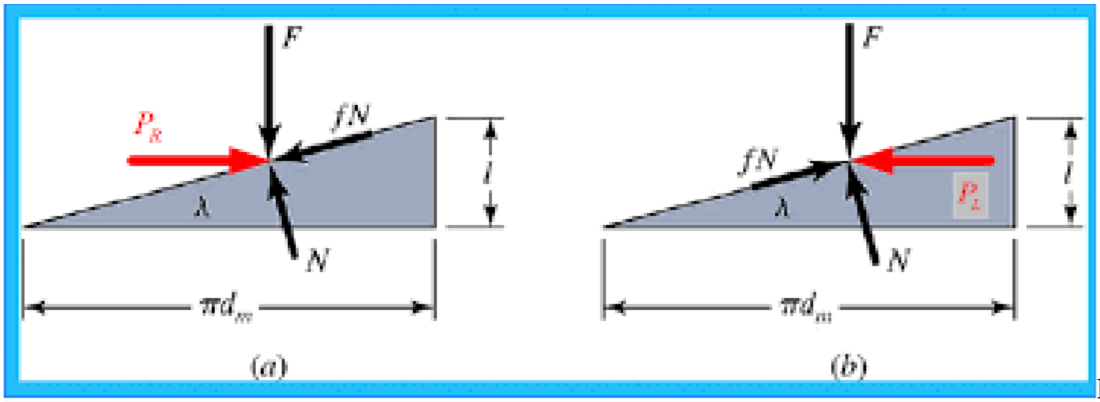

Fig. 6.1 Free Body Diagram

Considering Fig 6.1 (a) for opening the mechanism

$$\sum F_y = -F - fNsin\lambda + Ncos\lambda$$

$$N = \frac{(F + fNsin\lambda)}{cos\lambda}$$

$$\sum F_x = P_r - Nsin\lambda - fNcos\lambda = 0$$

$$P_r = \frac{F(sin\lambda - fcos\lambda)}{cos\lambda - fsin\lambda}$$

$$P_r = \frac{F(tan\lambda + f)}{1 - ftan\lambda}$$

$$P_r = \frac{F\left(\frac{l}{\pi d_m} + f\right)}{1 - \frac{fl}{\pi d_m}}$$

Torque required to move the load

$$T_R = \frac{F d_m}{2}\left(\frac{\frac{l}{\pi d_m} + f}{1 - \frac{fl}{\pi d_m}}\right)$$

$$\boxed{T_R = \frac{Fd_m}{2}\left(\frac{l + f\pi d_m}{\pi d_m - fl}\right)}$$

Considering image (b) for closing the mechanism,

Similarly, as for opening,

Torque

$$\boxed{T_L = \frac{Fd_m}{2}\left(\frac{\pi d_m - l}{\pi d_m + fl}\right)}$$

$$\frac{F}{cos\alpha} = Fsec\alpha$$

$$T_R = \frac{Fd_m}{2}\left(\frac{l + \pi f d_m sec\alpha}{\pi d_m - flsec\alpha}\right)$$

$$\boxed{F = \frac{2T_R}{d_m}\left(\frac{\pi d_m - flsec\alpha}{l + \pi f d_m sec\alpha}\right)}$$

We need the value Torque to find the force acting on the L-Bracket.
We can use the Power-Torque relation to find Torque

Power = Voltage x Current
= 12 V $\times$ 350 mA
= 12 V $\times$ 350 $\times$ 10^{-3}
= 4.2 W

$$\boxed{P = \frac{2\pi NT}{60}}$$

$$4.2 = \frac{2\pi \times 300 \times T}{60}$$

$T = \frac{2\pi \times 300}{60 \times 4.2}$ = 0.1336 Nm

Substitute this torque value in the force formula with other values.

$$F = \frac{2T_R}{d_m}\left(\frac{\pi d_m - fl\sec\alpha}{l + \pi f d_m \sec\alpha}\right)$$

$$F = \frac{2(0.1336)}{7 \times 10^{-3}}\left(\frac{\pi \times 7 \times 10^{-3} - (0.5 \times 0.002 \times 1.032)}{0.002 + \pi(0.5 \times 7 \times 10^{-3} \times 1.032)}\right)$$

$$F = 38.17\left(\frac{21.98 \times 10^{-3} - 1.032 \times 10^{-3}}{13.3 \times 10^{-3}}\right)$$

$$F = 38.17(1.575)$$

$$\boxed{F = 60.11 \text{ N}}$$

STRESS CALCULATIONS FOR DIFFERENT PARTS

(i) L-Bracket

Considering failure of rod under tension

Resisting area,

$$A = 24 \times 15 = 360 \text{ mm}^2$$

The force will be divided into 2 components. One hand of L-Bracket will have force value of

$P = F \times \cos 4\,5$
$= 60.11 \times \cos 4\,5$
$= 42.5041 \text{ N}$

Stress $\sigma_t = \frac{P}{A} = \frac{42.5041}{360} = 0.1180 \frac{\text{N}}{mm^2}$

(ii) Single eye end

Resisting area, $A = (d_1\text{-}d_2) \times t$ = 90 mm
[Considering failure under tension]

$$P = (d_1 - d_2)t - \sigma_t$$

$$\sigma_t = \frac{42.5041}{90} \frac{\text{N}}{mm^2}$$

(iii) Double eye end

The force is divided into two arms of the fork

Force $P = \frac{42.5041}{2} = 21.252$ N

Resisting area A = $(d_1-d_2)t \times 2 = (30-18)10 \times 2 = 120 \times 2$ mm

Stress $\sigma_t = \frac{P}{A} = \frac{21.252}{120\times2} \frac{\text{N}}{mm^2} = 0.0885 \frac{\text{N}}{mm^2}$

(iv) Knuckle Pin

$$\text{Resisting area} = \frac{\pi}{4} d^2 \times 2$$

$$= \frac{\pi}{4} \times 15^2 \times 2$$

$$= 353.25\, mm^2$$

Stress $\sigma_t = \frac{P}{A} = \frac{42.504}{353.25} = 0.1203 \frac{\text{N}}{mm^2}$

Ansys stress analysis

Mesh details

	Fork	Pin	Support
Aspect ratio	1.8043	2.12	2.301
Skewness	0.21	0.35	0.44
Type of mesh	Tetrahedron	Tetrahedron	Tetrahedron

Table 6.1 Mesh Details

(i) Double eye end

Mesh

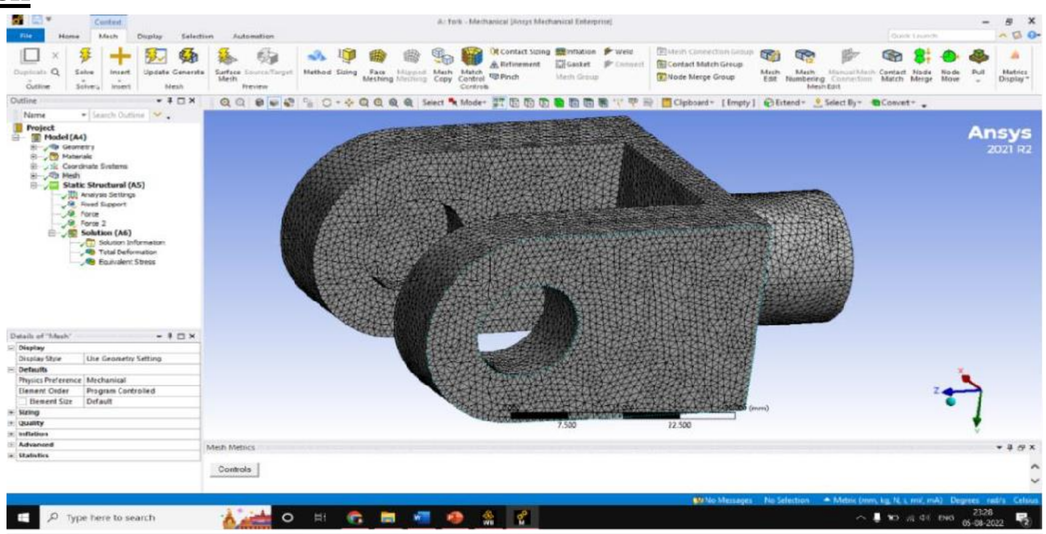

Fig. 6.1.1 Meshing of Double eye end

Boundary conditions

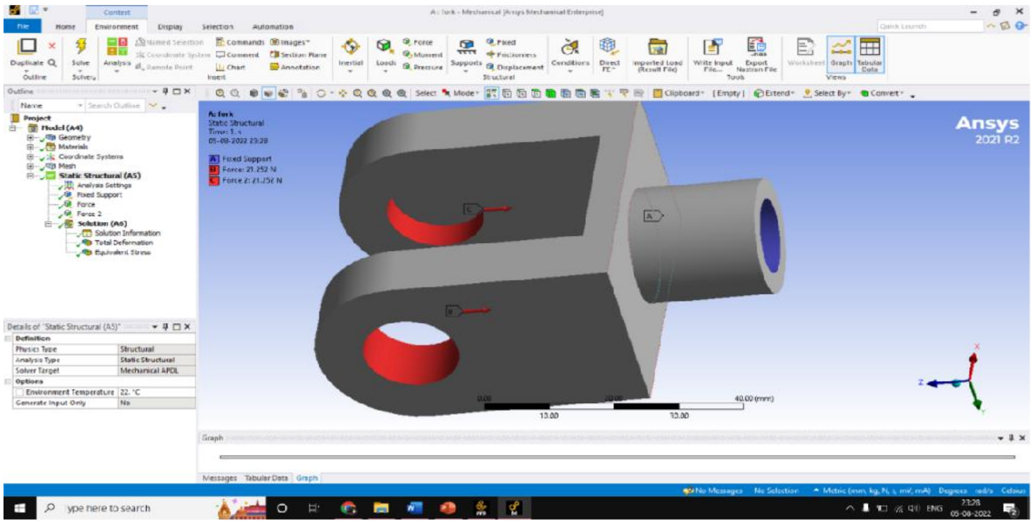

Fig. 6.1.2 Boundary Conditions of Double eye end

Stress

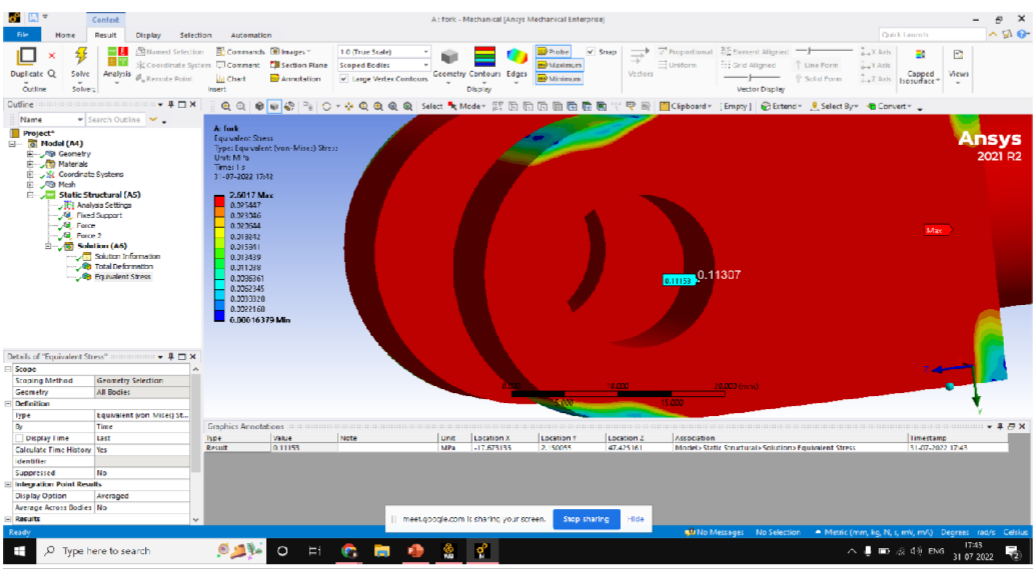

Fig. 6.1.3 Stress of Double eye end

(ii) L-Bracket

Mesh

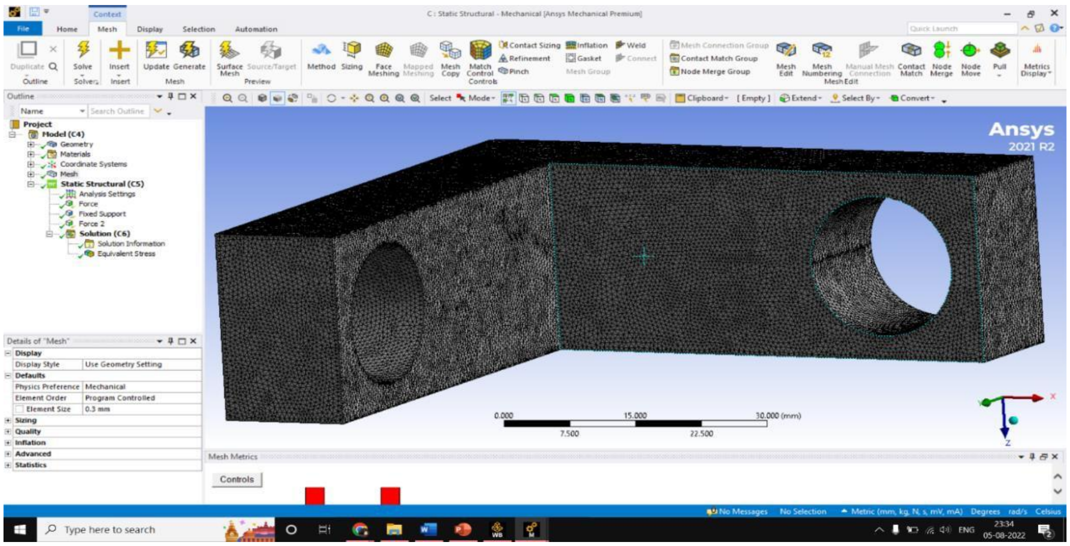

Fig. 6.2.1 Meshing of L-Bracket

Boundary conditions

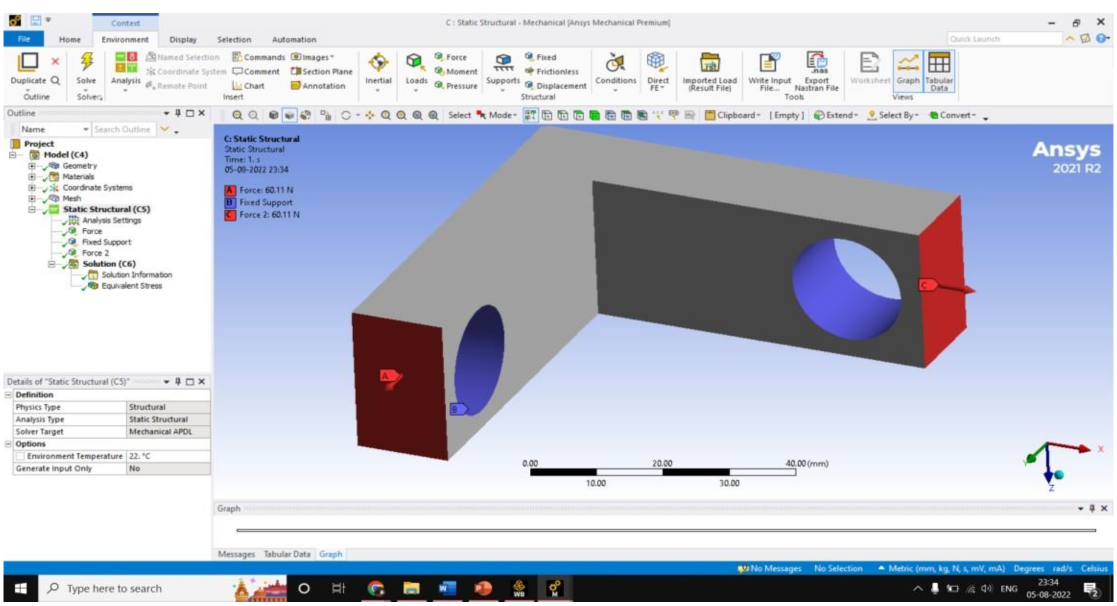

Fig. 6.2.2 Boundary Conditions of L-Bracket

Stress

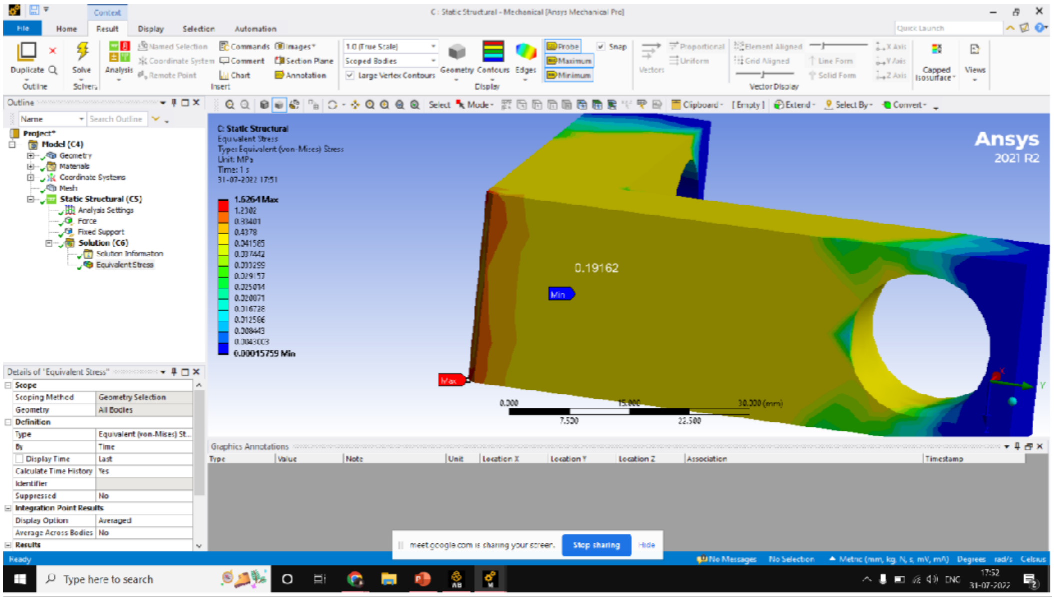

Fig. 6.2.3 Stress of L-Bracket

(iii) Knuckle Joint

Mesh

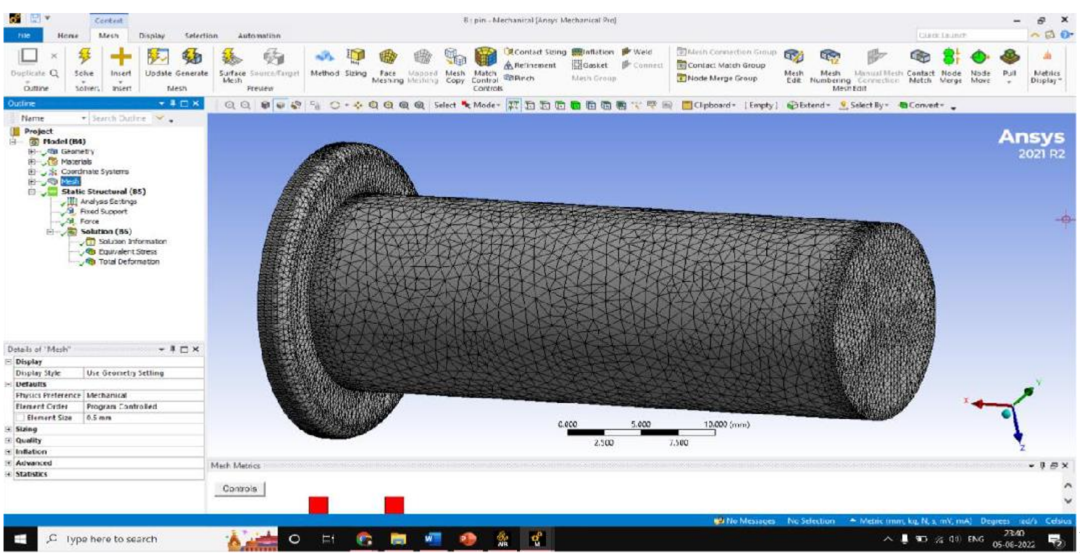

Fig. 6.3.1 Meshing of Knuckle Joint

Boundary conditions

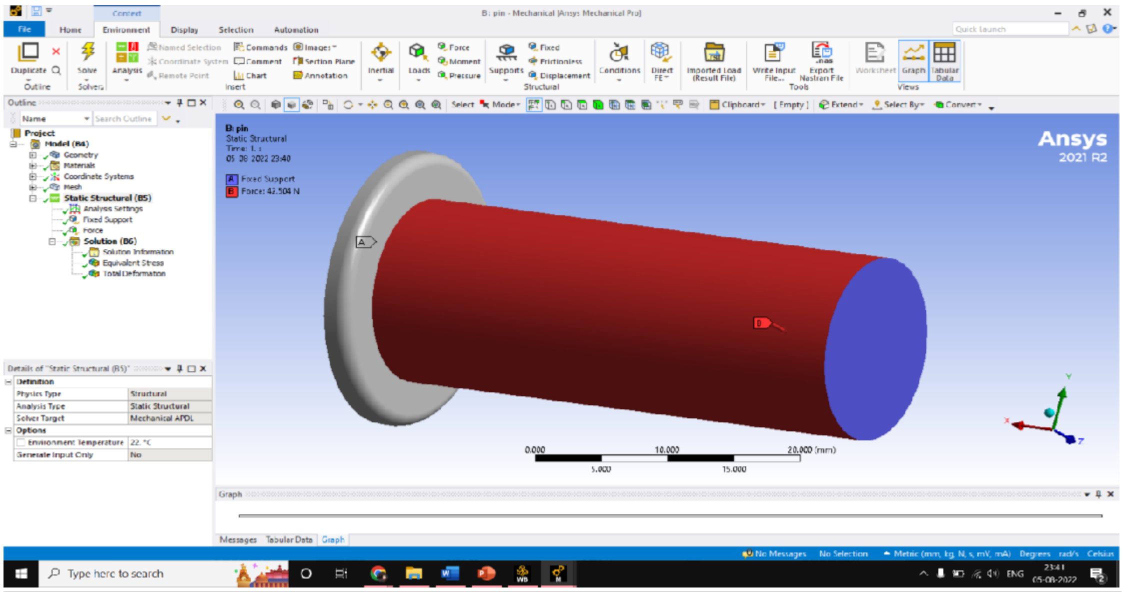

Fig. 6.3.2 Boundary Conditions of Knuckle Joint

Stress

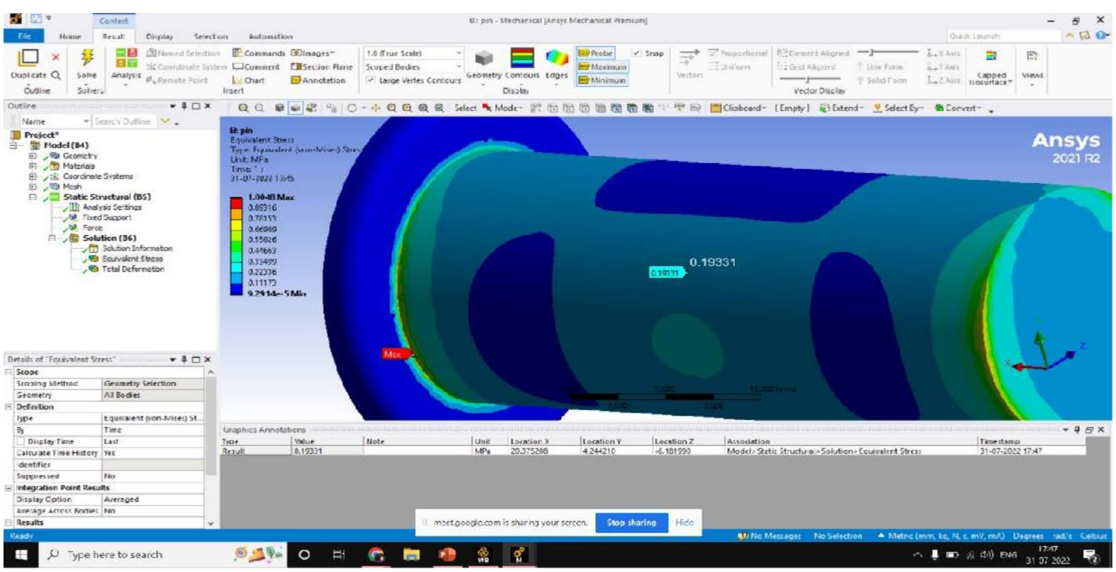

Fig. 6.3.3 Stress of Knuckle Joint

6.2) Results

Calculated results -comparison with ANSYS

Stress	Theoretical results ($\frac{N}{mm^2}$)	Ansys results ($\frac{N}{mm^2}$)
L-bracket	0.1180	0.19162
Single eye end	0.4722	0.19101
Double eye end	0.0885	0.11307
Pin	0.1203	0.19331

Table 6.2 Results Comparison

CONCLUSION

As we are aware of the risks and difficulties of space travel, sensitive instruments like photon receptors, camera lens, near-infrared spectrograph (NIRSpec) and many more are needed for deep space exploration. Our project as we have seen is based on the safe keeping and maintaining the proper conditions for functioning of above-mentioned devices. A heat shield acts as an extra layer between these instruments and the bizarre conditions experienced in space.

The James Webb Telescope revolutionized the use of a heat shield. In our case, we designed a system used to deploy a heat shield in a more economical and conventional manner. The method involved a different approach in the opening of the shield by using a lead screw as a linear actuator and reversing the bias of the motor would result in closing of the heat shield. Another intention of our design is to occupy as less payload volume as possible. As mentioned, the heat shield can close, this allows it to be reusable for future missions and/or during interplanetary flights.

A difficult task we faced was the involvement of meshing of the bevel gears, we dealt with it by adding extra c-clamps and reducing the cause of slip between the gears. For the frame, we selected a square frame design, this helped cover a larger area. The use of only one motor in our system reduces the total consumption of energy.

The materials we used included Aluminum 6061 for the frame, 3-D printed the supports and gears, and for the heat shield we used Kapton.

As a conclusion, our motive was to achieve ease in deployment and a more efficient cost-effective way heat shields can be affixed in future launch vehicles and satellites.

REFRENCES

- Evans T.A., Lang R.J., Magleby S.P., Howell L.L. (2015), Rigidly Foldable Origami Gadgets and Tessellations, Royal Society Open Science, 2015.
- Gantes C. J. (2001), Deployable Structures: Analysis and design, WIT Press, Southampton.
- Hoberman C. (2004), Retractable Structures Comprised of Interlinked Panels, US Patent 6739098.
- Kripa K. Varanasi, Samir A. Nayfeh (2014), The Dynamics of Lead-Screw Drives: Low-Order Modeling and Experiments, Massachusetts Institute of Technology Cambridge, Massachusetts.
- Robert Lipsett, Why Lead Screws are the Best Fit for Many Linear Motion Applications - and How to Rightly Apply Them, Thomson BSA Thomson Industries, Inc. San Jose, CA.
- Yashashri Dhaware, Prachi Palkuntwar, Harshal Narkhede, Rushabh Meher, Priyanka Chavan, Bakhtiyar Gandevia (2019), Review on Comparative Analysis of Ball Screw & Lead Screw, Pimpri-Chinchwad College of Engineering and Research, Pune.
- DuPont™ Kapton® Summary of properties, kapton.com.
- Adaptable Deployable Entry and Placement Technology (ADEPT), NASA
- Wenjing Jin, Yan Chen, Jay Lee (2013), Methodology for ball screw component health assessment and failure analysis, Madison Wisconsin, USA.
- Supriya Kulkarni, Prithviraj Kajale and D U Patil (2015)., Recirculating ball screw.